The quest for new thermoluminescence and optically stimulated luminescence materials Needs, strategies and pitfalls

Yukihara, Eduardo G.; Bos, Adrie J.J.; Bilski, Paweł; McKeever, Stephen W.S.

DOI
10.1016/j.radmeas.2022.106846

Publication date
2022

Document Version
Final published version

Published in
Radiation Measurements

Radiation Measurements 158 (2022) 106846

Contents lists available at ScienceDirect

Radiation Measurements

journal homepage: www.elsevier.com/locate/radmeas

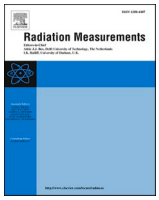

The quest for new thermoluminescence and optically stimulated luminescence materials: Needs, strategies and pitfalls

Eduardo G. Yukihara [a,*], Adrie J.J. Bos [b], Paweł Bilski [c], Stephen W.S. McKeever [d]

[a] Department of Radiation Safety and Security, Paul Scherrer Institute, PSI, 5232, Villigen, Switzerland
[b] Department of Radiation and Technology, Faculty of Applied Sciences, Delft University of Technology, Delft, the Netherlands
[c] Institute of Nuclear Physics, Polish Academy of Sciences, PL-31-342, Kraków, Poland
[d] Department of Physics, Oklahoma State University, Stillwater, OK, 74078, USA

ARTICLE INFO

Keywords:
Thermoluminescence
Optically stimulated luminescence
Dosimetry
Synthesis

ABSTRACT

The quest for new materials for thermoluminescence (TL) and optically stimulated luminescence (OSL) dosimetry continues to be a central line of research in luminescence dosimetry, occupying many groups and investigators, and is the topic of many publications. Nevertheless, it has also been a research area with many pitfalls, slow advances in our understanding of the luminescence processes, and rare improvements over existing materials. Therefore, this paper reviews the status of the field with the goal of addressing some fundamental questions: Is there a need for new luminescence materials for TL/OSL dosimetry? Can these materials be designed and, if so, are there strategies or rules that can be followed? What are the common pitfalls and how can they be avoided? By discussing these questions, we hope to contribute to a more guided approach to the development of new luminescent materials for dosimetry applications.

1. Introduction

Thermoluminescence (TL) and Optically Stimulated Luminescence (OSL) are phenomena widely used in radiation dosimetry and applied in different fields, such as personal and environmental dosimetry, medical dosimetry, imaging of ionizing radiation dose, archeological and geological dating and assessment of the severity of radiation accidents (McKeever, 1985; McKeever et al., 1995; Chen and McKeever, 1997; Bøtter-Jensen et al., 2003; Chen and Pagonis, 2011; Yukihara and McKeever, 2011; Yukihara et al., 2022b). Besides dosimetry applications, TL materials have also been explored as particle temperature sensors (Talghader et al., 2016; Yukihara et al., 2018), and OSL materials have been examined as rechargeable persistent phosphors for bioimaging applications (Xu et al., 2018). OSL materials are also used as photostimulable phosphors in computed radiography (Leblans et al., 2011).

In such TL/OSL applications a key role is played by the luminescent material. Since the work on TL dosimetry materials by Daniels and colleagues and on OSL dosimetry materials by Antonov-Romanovskii in the 1950s (Daniels et al., 1953; Antonov-Romanovskii et al., 1955) there has been a continuous and extensive search for the "ideal" luminescent material that exhibits a linear dose-response relationship over the widest possible dose range, a high sensitivity, along with good neutron/gamma discrimination, tissue equivalency, reproducibility, and stability of the luminescent signal. With the expansion of TL/OSL to applications beyond personal and environmental dosimetry, the concept of the "ideal" material also has to be revised according to new applications. The historical development, properties and uses of various TL materials have been summarized in McKeever et al. (1995). Since then other reviews can be found for TL (Bhatt and Kulkarni, 2014) and for OSL materials (Pradhan et al., 2008; Nanto, 2018; Yanagida et al., 2019; Yuan et al., 2020).

Although many materials show promising TL/OSL properties, few have been used routinely or commercially in dosimetry (see Table 1). Available TL dosimetric materials are mostly limited to doped compounds of fluorides (LiF, CaF_2), simple oxides (Al_2O_3, BeO, MgO), borates (MgB_4O_7, and $Li_2B_4O_7$) and sulfates ($CaSO_4$). In the case of OSL, only two OSL materials are used in commercial dosimetry systems: Al_2O_3:C and BeO. Both are highly sensitive to ionizing radiation. For computed radiography other OSL materials such as BaFBr:Eu and CsBr:Eu are also available (Leblans et al., 2011; Nanto, 2018), but these were designed not for dosimetry, but for X-ray imaging, and have high effective atomic numbers ($Z_{eff} \geq 30$–50). Several other materials have been investigated for OSL dosimetry (Pradhan et al., 2008; Oliveira and

* Corresponding author.
E-mail address: eduardo.yukihara@psi.ch (E.G. Yukihara).

https://doi.org/10.1016/j.radmeas.2022.106846
Received 21 March 2022; Received in revised form 26 July 2022; Accepted 16 August 2022
Available online 20 August 2022

Table 1
Summary of TL and OSL materials most used in dosimetry. Most of the data are from McKeever et al. (1995) with a few updates, as indicated with the additional references; for OSL properties, see (Bøtter-Jensen et al., 2003; Yukihara and McKeever, 2011). The linearity ranges are those summarized in ISO/ASTM 51956 (ISO/ASTM, 2013b), also based on data from McKeever et al. (1995).

Material	Technique	Z_{eff} (host)	Comments
LiF:Mg,Ti	TL	8.3	Widely used in individual and area monitoring, and in medical dosimetry. TL sensitivity and curve shape influenced by aggregated defects that change with annealing and time. Linear up to 1 Gy, supralinear 1 Gy–10^3 Gy.
LiF:Mg,Cu, P	TL	8.3	High sensitivity, but cannot be heated above 240 °C without loss of sensitivity. Linear up to 10 Gy, then sublinear. High-temperature TL can be used >10^3Gy.
LiF:Mg,Cu, Si	TL	8.3	Kim et al. (2022)
CaF_2:Mn	TL	16.9	Linear up to 10 Gy, supralinear up to 10^3 Gy.
CaF_2:Dy	TL	16.9	Linear up to 6 Gy, supralinear up to 500 Gy.
CaF_2:Tm	TL	16.9	Linear up to 1 Gy, supralinear up to 10^4 Gy.
Al_2O_3:C	TL/OSL	11.3	High TL and OSL sensitivity, broad, complex single TL peak. Linear up to 1 Gy, supralinear up to 30 Gy.
Al_2O_3:C, Mg	TL/OSL	11.3	Higher concentration of shallow traps in comparison with Al_2O_3:C and more aggregated defects.
Al_2O_3:Mg, Y		11.3	Linear up to 10^4 Gy.
BeO	TL/OSL	7.2	Low TL sensitivity; high OSL sensitivity. Linear up to 1 Gy, supralinear up to 100 Gy.
MgO	TL	10.8	Linear up to 10^4 Gy.
$CaSO_4$:Dy	TL	15.6	Linear up to 10 Gy, supralinear up to 10^3 Gy.
$CaSO_4$:Tm	TL	15.6	Linear up to 10 Gy, supralinear up to 10^3 Gy.
$Li_2B_4O_7$: Mn	TL	7.3	Linear up to 100 Gy, supralinear up to 10^4 Gy.
$Li_2B_4O_7$: Mn,Si	TL	7.3	Danilkin et al. (2006)
$Li_2B_4O_7$: Cu	TL	7.3	Linear up to 10^3 Gy.
MgB_4O_7: Dy	TL	8.5	Linear up to 50 Gy, supralinear up to 5 × 10^3 Gy.
MgB_4O_7: Tm	TL	8.5	Linear up to 50 Gy, supralinear up to 5 × 10^3 Gy.

Baffa, 2017; Souza et al., 2017; Sądel et al., 2020a), but have not yet being routinely used in such applications.

With Table 1 in mind, is there a need for new luminescence materials for TL/OSL dosimetry? If so, can these materials be designed and are there strategies or rules that can be followed in doing so? What are the common pitfalls to achieving optimum design and can they be avoided?

The objective of this review is to address the questions above. We will first discuss the general requirements for dosimetry, how the existing materials satisfy (or not) the requirements, and which new demands on material properties are arising. We will then discuss possible strategies to develop new materials and the limitations of these approaches. Finally, we will discuss pitfalls that have been encountered in the literature. By discussing these questions, we hope to contribute to a more guided approach to the development of new luminescent materials for dosimetry applications. Given the large literature on the subject, not all materials or cases can be discussed and the examples presented here rely on the authors' experience.

2. General requirements and the need for materials

2.1. General requirements

The desirable properties of a TL or OSL dosimeter depend on the particular application, and some can be highlighted.

2.1.1. High sensitivity

High sensitivity to ionizing radiation is particularly important in fields in which low doses are involved, e.g. environmental, individual and area monitoring, and for some radiodiagnostic techniques. It is also important if the amount of material that can be used is limited, for example if the goal is to produce films for 2D dosimetry in radiotherapy, or where small dosimeters are needed in order to not disturb the radiation field or to avoid volume averaging in regions of steep dose gradients. For areas involving high doses, other factors may be more relevant (e.g., reproducibility, dose- and energy-response relationship, saturation level, stability).

There is no requirement specifically on the sensitivity of the luminescent materials, only on the performance of the entire dosimetry system (IEC, 2020). This, in turn, depends on the choice of signal (TL or OSL, peak intensity or area), intrinsic sensitivity of the material, amount of material contained in the detector, number of detectors used for the dose evaluation, readout approach and scheme, and detection efficiency of the reader, including the signal reduction that can occur due to the use of optical filters, signal processing and discrimination. The term '"detector" is used to mean the sensitive part of the dosimeters, that is, a specific quantity of TL or OSL material in a specific physical form (IEC, 2020; Yukihara et al., 2022b).

It is useful to compare the sensitivity of a material with well-known TL/OSL materials used commercially in dosimetry systems, keeping in mind that the factors mentioned above can influence the sensitivity measurement (see also Section 4.1). The sensitivity of a specific material, e.g. LiF:Mg,Ti, can of course vary with the manufacturer - there is no "gold standard". Nevertheless, such comparisons are useful to evaluate the potential applications of new materials.

Fig. 1a shows a few examples of TL detectors (TLDs) and OSL detectors (OSLDs) in typically available shapes, followed by a comparison of the TL signals acquired at a constant heating rate (Fig. 1b and c), or OSL signals acquired at constant stimulation intensity (Fig. 1d). These figures compare the output of each detector, that is, the intensity is a result of the type and amount of material in each detector. The data are provided only as a qualitative comparison of the TL/OSL curve shapes and as an order-of-magnitude comparison of the intensities from the various detectors, since the actual intensities can vary due to the various parameters used in the measurements (detection filters, batch, manufacturer, dopant concentration, material's transparency, etc.).

2.1.2. Linear dose-response relationship

A linear dose-response relationship in the dose region of interest simplifies the dosimetry by avoiding the need for non-linearity correction factors or multiple calibration points. Above a dose of a few grays most TL/OSL materials exhibit either supralinear behavior (a response higher than that expected by extrapolating from the low-dose region) or sublinear behavior. Sublinearity can occur as the material approaches saturation, or as desensitization effects dominate at high doses (Chen and McKeever, 1994; Yukihara et al., 2003, 2004; McKeever, 2022).

Supralinearity not only influences the dose-response relationship; it is inherently associated with a change in the material sensitivity, which can be observed even at low doses, therefore influencing the repeatability of the measurements. One of the explanations for such sensitivity change is the filling of deep electron and hole traps that compete for charge capture. Resetting the sensitivity may require annealing the materials to a temperature sufficiently high to empty such deep traps (Chen and McKeever, 1997; Yukihara et al., 2003). High precision dosimetry without annealing can still be achieved in these conditions, but a careful protocol that takes into account the material's properties must be developed (Yukihara et al., 2005; Wintle and Murray, 2006).

2.1.3. Flat relative photon energy-response relationship

For personal or medical dosimetry the measured signal must be related to absorbed dose in the body of a person (ICRU, 1993; Andreo et al., 2017). In that case, a desirable property is a TL/OSL response as

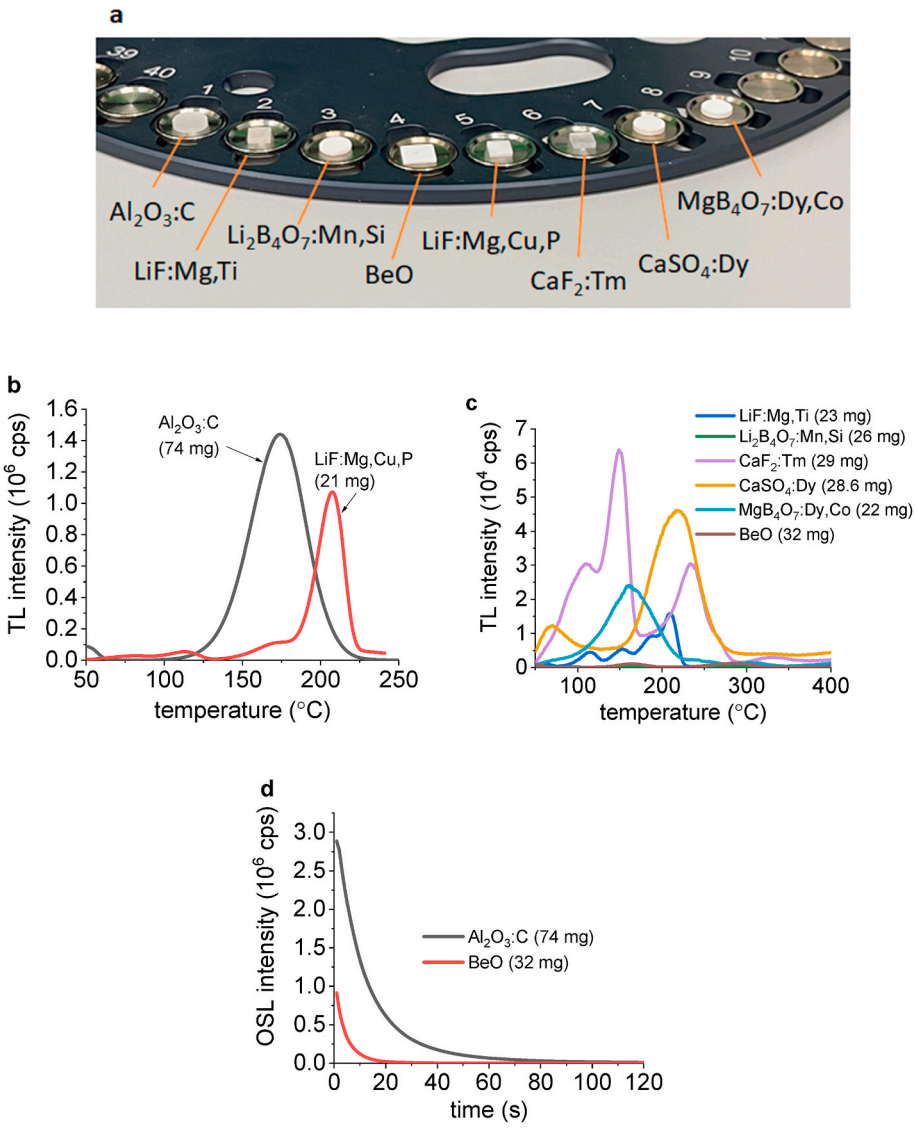

Fig. 1. (a) Examples of various TL and OSL materials; (b) TL curves of Al_2O_3:C and LiF:Mg,Cu,P; (c) TL curves of the other TL materials; and (d) OSL curves of Al_2O_3:C and BeO. All TL curves were measured at 1 °C s^{-1} using a wideband blue filter (Schott BG 39 + Schott BG 25 + Schott KG 3), except for BeO, for which a Hoya U340 + Delta BP 365/50 EX filter combination was used. The OSL from Al_2O_3:C was measured using green stimulation (525 nm, 50 mW cm^{-2}) and a Schott BG 3 + Delta BP 365/50 EX filter combination, whereas the OSL from BeO was measured using blue stimulation (458 nm, 80 mW cm^{-2}) and a Hoya U340 + Delta BP 365/50 EX filter combination. All data were obtained using a Lexsygsmart reader (Freiberg Instruments GmbH, Freiberg, Germany). The detectors were irradiated with an absorbed dose to water of approximately 50 mGy using a beta $^{90}Sr/^{90}Y$ source; the actual dose can vary with the thickness and composition of the materials.

function of the photon energy of the absorbed radiation (photon energy-response relationship) which mimics that of the medium of interest (e.g. human tissue). The photon energy-response relationship, expressed as the ratio between the dose evaluated by the dosimeter and the quantity of interest as a function of the photon energy, should be flat and identical to one. Values higher than one mean that the dosimeter over-responds to the photon field, whereas values lower than one mean that the dosimeter under-responds to the photon field.

A flat relative photon energy-response relationship is mostly important for low energy X-rays, the photon energy range in which the photoelectric effect dominates. Since the photoelectric effect typically has a dependence with Z^4 (Attix, 2004), where Z is the atomic number of the material, differences in atomic number between the material of the detector and of the medium result in different absorbed doses when both are exposed to the same photon field. Even in high-energy photon fields, in which the Compton effect dominates and the interaction cross-section from the materials are similar, part of the energy deposited in the detectors may come from low energy X-rays from scattering of the primary beam.

The photon energy response is predominantly determined by the host material and can be represented by the effective atomic number Z_{eff} (Bos, 2001a; Attix, 2004). The Z_{eff} from LiF is 8.3, that from Al_2O_3 is 11.3, and that of tissue is around 7.6 (Bos, 2001a). Materials that approach the Z_{eff} from tissue are called "tissue equivalent". The higher the discrepancy between the Z_{eff} from the material and the medium of interest, the higher the over- or under-response of the material with respect to that medium.

Tissue equivalency is mostly important if the detectors are used directly, for example by placing them on a patient or phantom for investigation of doses in radiodiagnostics (Scarboro et al., 2019). In general, the TL/OSL materials based on LiF, $Li_2B_4O_7$, MgB_4O_7 and BeO are more tissue equivalent than other materials noted in Table 1.

However, this is not to say that materials with higher effective atomic numbers cannot be used in personal dosimetry, Al_2O_3 with Z_{eff} = 11.3 being an example of a widely used dosimetric material that is not perfectly tissue equivalent. If the detectors are to be used on a badge containing filters that can change the detected radiation field, often combined with other detectors or filters, then the overall requirements are on the final dose estimates of the entire dosimetry system, not just the material (IEC, 2020). Commercial systems are able to combine signals with different photon energy responses to estimate the mean energy of the radiation field and obtain a "flat" energy-response relationship (Yukihara et al., 2022b). Nevertheless, such approaches may increase the size of the dosimeter badge and affect its angle dependence. The issues involved in using high Z_{eff} materials in dosimetry are discussed by Chumak and colleagues (Chumak et al., 2017).

2.1.4. High reproducibility

Reproducibility of a TL or OSL measurement can depend on both material and experimental factors, such as the reproducibility of the irradiation and of the readout system. Furthermore, as in the case of the sensitivity, reproducibility requirements apply to the final dose estimates of the whole dosimetry system. The requirement in individual monitoring (IEC, 2020) is a standard deviation of ~5–15% and is particularly less stringent when involving low doses. In radiation therapy, however, the requirement is more strict, with a standard deviation of <5% and a confidence interval of two standard deviations (with a coverage factor of 2) for the entire dose estimate (IAEA, 2000).

A material for which the TL/OSL signal is independent of its thermal or dosimetric history will contribute to a high reproducibility, simplifying the entire dosimetry and quality assurance processes and ultimately improving the measurement precision.

2.1.5. High stability

It is desirable to have a material with: (a) a sensitivity that is stable over time – i.e. the signal does not depend on how long after preparation the irradiation took place; and (b) a signal that is stable over time after irradiation –i.e., one that does not depend on the time between irradiation and readout. Variation in the sensitivity with time is called "aging", whereas the variation in the signal after irradiation is called "fading". As an example, such effects have been observed in LiF:Mg,Ti (Ptaszkiewicz, 2007; Luo, 2008; Sorger et al., 2020).

The TL signal stability is typically associated with the temperature of the respective TL peaks, the stability increasing with the temperature of the peak in a first approximation. Therefore, unless so-called anomalous fading takes place (Wintle, 1973), signals at temperatures higher than 150–200 °C should have thermal stability sufficient for personal dosimetry, with fading of less than approximately 10%/month, as required by international standards for passive dosimetry (IEC, 2020).

The OSL signal stability is more complicated. Because light can stimulate the signal associated with different traps having different thermal stabilities, the OSL signal stability will be a combination of the stability of those signals. For example, the OSL signal may exhibit a short-term decay due to the decay of shallow traps (traps that are unstable at room temperature), followed by a more stable or slow-decaying signal due to the contribution from traps that are more stable at room temperature. For this reason, OSL dosimeters often should not be read out immediately after irradiation (Kry et al., 2020). Alternatively, a thermal treatment (pre-heat) to a temperature sufficient to empty the shallow traps without affecting the main dosimetric traps can be applied.

Corrections for fading can be implemented (Kry et al., 2020), but any correction will contribute to the uncertainty of the measurements. This can be critical in high precision applications, such as dosimetry in radiotherapy.

2.1.6. Reusability

Reusability of detectors was one of the advantages that, in the past, led to replacing film dosimetry with TLDs. Although TL/OSL materials in powder form may also be applied as disposable, one-time detectors, in most applications they are expected to be fully reusable.

In the case of TLDs, the high temperature during readout or annealing may be the factor limiting their reusability. This is, for example, the situation with LiF:Mg,Cu,P, the TL properties of which deteriorate when heated above 240 °C (Tang, 2000). Even if this limit is kept, a gradual decrease of sensitivity with repeated use is sometimes observed (Sáez-Vergara and Romero, 1996). In the case of OSLDs, the reusability may be limited if complete bleaching of a detector (emptying the trapping sites by illumination) cannot be achieved within a reasonable time, leading to an accumulation in the residual signal with usage. In high-dose measurements, the possibility of radiation damage should be considered (Bilski et al., 2008).

Even when the detectors are re-useable, sensitivity changes with dose history and annealing introduce additional uncertainties. In the case of OSLDs, for example, special readout protocols have been developed to achieve uncertainties of the order of 1.0% or less (Yukihara et al., 2005). Such protocols require specialized research equipment capable of reading the OSL, irradiating the detectors with a reference dose, and reading them again.

2.1.7. High neutron sensitivity

For use in neutron dosimetry, TL/OSL materials with a high concentration of ^{6}Li or ^{10}B are desired, because of the high neutron capture cross-section of these isotopes (Knoll, 2000). ^{155}Gd and ^{157}Gd have also been used in neutron detectors, but for luminescence dosimetry they are not so effective. This is because the products of the neutron capture reaction are gammas, conversion electrons and X-rays, most of which will escape the detector and deposit their energies elsewhere (Mittani et al., 2007). In the case of the ^{6}Li(n,α) and the ^{10}B(n,α) neutron capture reactions, on the other hand, the products are heavy particles (^{3}H, ^{4}He or ^{7}Li, depending on the reaction), which deposit the energy locally in the detector (Knoll, 2000).

Since the TL/OSL materials are also sensitive to gamma radiation, it is important to have a good discrimination between neutrons and gammas. This can be done by using two detectors, one having a high neutron sensitivity (e.g., prepared with ^{6}Li) and one having a low neutron sensitivity (e.g., prepared with ^{7}Li). The difference between their signal, taking into account individual sensitivities, is proportional to the neutron dose, whereas the gamma dose is given by the neutron-insensitive detector.

Because the energy deposited by the products of the neutron-capture reactions and the gammas have different ionization densities, the TL/OSL signals due to neutrons and gammas can be different: different ratios between TL peaks or between OSL emission bands. These could in principle be used to further improve the neutron/gamma discrimination (Noll et al., 1996).

2.1.8. Other requirements

In addition to the typical requirements listed above, new developments particularly in radiotherapy pose an increasing challenge for TL/OSL materials.

In ion beam therapy and space dosimetry, the effect of ionization quenching, a reduction in the luminescence efficiency with particle LET, has been a major disadvantage of TL/OSL detectors (Kalef-Ezra and Horowitz, 1982; Olko, 2002; ICRP, 2013).

The response of luminescence detectors is known to decrease with increasing particle LET, a phenomenon called ionization quenching, because it is related to the high ionization densities created by the passage of heavy charged particles through the detector. In short, the energy deposited by the passage of the heavy charged particles saturate the detector within the particle track and, therefore, a higher energy deposition (higher LET particle) does not lead to an increase in the luminescence signal. This results in an under-response (quenching) with increasing LET. This LET-dependence of the luminescence efficiency introduces a complexity for the precise dosimetry in ion beam therapy, since the detector response will depend on the LET spectrum of the radiation at the point of measurement, which can only be estimated with the assistance of Monte Carlo simulations.

Although it is unlikely that TL/OSL materials can be developed with constant efficiency for the wide range of linear LET values encountered in space, as high as 10^{3} keV/μm, it has been demonstrated that materials with reduced quenching can be developed for narrow LET ranges, such as those encountered in proton therapy (Yukihara et al., 2022a).

The use of high dose rates (>10^{6} Gy/pulse) in radiotherapy (FLASH therapy) (Vozenin et al., 2019) creates a demand for detectors that are dose rate independent. Some studies have demonstrated that TL/OSL materials have the potential to fulfill this requirement (Karsch et al., 2012; Christensen et al., 2021), but experiments are still needed for confirmation (Horowitz et al., 2018).

The combination of magnetic resonance imaging (MRI) and radiotherapy in MRI-guided radiotherapy (Jaffray et al., 2010) also introduces the requirement of measuring doses precisely in the presence of strong magnetic fields. There is also evidence that TL/OSL materials could perform well in these conditions (Spindeldreier et al., 2017; Shrestha et al., 2020b).

These are just a few examples of how the technical developments place increasingly demanding dosimetry requirements. New applications may lead to new sets of requirements.

2.2. The need for new TL/OSL materials

In this Section we discuss the areas in which new TL/OSL materials are needed.

2.2.1. TL

The range of host/dopant combinations found in Table 1 provides a wide variety of properties, including different TL curve shapes, emission spectra, dose-response curves, effective atomic number and fading.

LiF:Mg,Ti remains a "reference dosimeter" in individual monitoring and medical applications because of its availability, balance between tissue equivalency, sensitivity to ionizing radiation, insensitivity to light, control of neutron sensitivity (^{6}LiF:Mg,Ti versus ^{7}LiF:Mg,Ti), and well-defined TL peaks that facilitates the analysis and the isolation of stable TL peaks. Moreover, due to its widespread use, it has also been the subject of numerous studies over the decades. The TL curve consists of several peaks, the main ones of interest for dosimetry being located at ~230 °C (the exact temperature varies with the heating rate) (McKeever et al., 1995).

One of LiF:Mg,Ti disadvantages is the variation in the TL curve and sensitivity as a function of the annealing regime (temperature, time, cooling rates, etc.) and time since annealing (Ptaszkiewicz, 2007; Luo, 2008; Sorger et al., 2020). This is caused by the fact that the TL peaks of interest for dosimetry are linked to impurity-vacancy pairs associated as trimers, and aggregations/disaggregation processes are influenced by time and temperature (McKeever et al., 1995; Horowitz and Moscovitch, 2013). Another disadvantage is the supralinear behavior in the 1–1000 Gy region, before sublinearity and/or saturation.

LiF:Mg,Cu,P has a sensitivity >20 times higher than LiF:Mg,Ti, but the TL signal saturates at lower doses and the annealing cannot be at temperatures higher than 240 °C. This temperature is not sufficient to empty the TL peaks that appear at temperatures higher than that, leading to an increased background with dose (McKeever et al., 1995). Nevertheless, LiF:Mg,Cu,P has been widely used in dosimetry (Moscovitch, 1999).

Al_2O_3:C is a high sensitivity TL material, particularly for environmental dosimetry applications, with dominant TL peak at ~180 °C, peak emission at 420 nm and low fading (Akselrod et al., 1990). The main disadvantage for TL dosimetry is the light sensitivity, which requires the detectors to be protected from light during use and handling (Moscovitch et al., 1993). The light sensitivity is actually what makes this material an excellent OSL dosimeter (see Section 2.2.2).

BeO is also a material with known TL properties (Tochilin et al., 1969), but which has a poor sensitivity in the TL mode due to thermal quenching of the signal (Bulur and Yeltik, 2010; Yukihara, 2011). The material has three main TL peaks, the most intense being at ~200 °C. Higher sensitivities can be achieved in OSL mode, which finally made the material commercially viable as a dosimeter (see Section 2.2.2).

As one can see, several TL materials are available covering most applications in personal, environmental and medical dosimetry. Probably for this reason, few new materials have gained traction in the last 25 years, as seen by the fact that most of the materials in Table 1 are the same as those listed in McKeever et al. (1995). From an economic point of view, laboratories may have an interest in developing their own detectors; this is why even natural materials are sometimes used in routine dosimetry (Umisedo et al., 2020). Apart from that, the need for new TL materials is justified only in specific cases, some of which are discussed below.

Higher sensitivity. Although the range of TL sensitivities from commercial TLDs is sufficient for environmental and personal dosimetry, materials with higher sensitivity could allow a reduction of material used in each detector, the development of readers using simpler light detectors, or could enable new applications requiring micrometer-sized particles, e.g. for particle temperature sensing (Armstrong et al., 2018).

Improved precision. The precision in TL dosimetry is often limited by effects such as the dependence of the TL sensitivity and curve shape on thermal history, the presence of supralinearity or saturation in the response of the detector to absorbed dose, the photon-energy dependence, etc., all of which are seen in most of the TL materials described so far. Therefore, precision in TL dosimetry could be improved with a material that has a wide range of linear response to dose and a TL sensitivity and curve shape that are extremely reproducible regardless of the annealing conditions or the time elapsed since annealing or irradiation. Fig. 2a illustrates a typical dose-response curve and the response of an ideal material with a wider range of linearity and saturation at higher doses (since saturation is inevitable).

Higher saturation doses. TL dosimetry becomes increasingly complicated and impractical once the doses are in the supralinear region of the dose response, or impossible if saturation is reached. Materials with higher saturation doses could make the dosimetry of high doses more practical, for example for radiation processing, including irradiation of blood products, production of sterile insects, sterilization of medical products, food irradiation, modification of polymers and other industrial processes, where doses up to 1 MGy can be used (ISO/ASTM, 2013a). As seen in Table 1, most of the TL materials show supralinearity for doses >1 Gy–100 Gy, depending on the material, which complicates the calibration procedure, and few materials are capable of measuring above 10^4 Gy. Therefore, TL materials with extended linearity ranges and saturation at doses up to 10^6 Gy are desired. Nevertheless, one must demonstrate the advantage of a TL system over other currently used dosimetry technologies, such as alanine and polymethylmethacrylate (PMMA) dosimetry systems (ISO/ASTM, 2013a, b).

Reduced ionization quenching. As discussed in Section 2.1.8, most TL and OSL materials exhibit ionization quenching. Although this cannot be avoided, materials with higher saturation doses would in principle exhibit reduced ionization quenching (Olko and Bilski, 2020; McKeever, 2022), possibly reducing the need for LET-dependent correction factors. This has been demonstrated in the case of OSL (Yukihara et al., 2022a), indicating the potential of improving the precision in ion beam therapy dosimetry. Fig. 2b illustrates the typical relative luminescence efficiency versus LET for TL/OSL materials; an improved response would extend the LET range in which the luminescence efficiency is closer to ideal; ultimately a reduction in efficiency is inevitable due to saturation of the traps within the particle tracks.

Multiple TL peaks. TL materials with high sensitivity and multiple TL peaks that are not light sensitive are of interest for particle temperature sensing applications (Talghader et al., 2016; Yukihara et al., 2018). The more TL peaks available, the wider the temperature range of application of the TL materials. Fig. 2c represents an ideal material for temperature sensing, whose TL curve consists of a superposition of well-defined first-order TL peaks covering a wide temperature range. In dosimetry, multiple TL peaks with different responses to photons or particles could provide more information to improve the dosimetry. In the past, there were several attempts to use TLDs for distinguishing different radiation types. Some success was achieved for this purpose by exploiting the ratio of TL peaks in CaF_2:Tm (Hajek et al., 2008; Muñoz et al., 2015) and LiF:Mg,Ti (Schöner et al., 1999; Berger et al., 2002).

In the discussion above, there are two points to keep in mind: First, the properties above are not the only ones to be considered; the complete set of requirements for each specific application must be taken into account. One may have a material with an extremely high sensitivity, but which fades quickly or which has a strong photon energy response

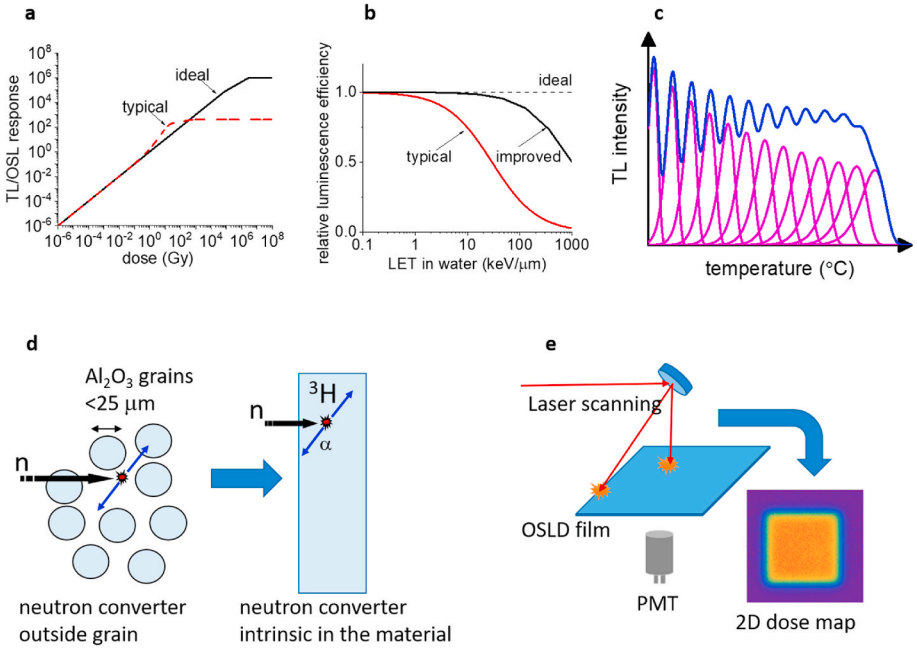

Fig. 2. Examples of some areas in which new TL/OSL materials are needed: (a) extended linear dose response with higher sensitivity and higher saturation doses; (b) no or smaller ionization quenching and no over-response (efficiency >1) at intermediate LET values; (c) ideal TL curve for temperature sensing applications (blue), consisting of multiple TL peaks uniformly distributed over a wide temperature range; (d) intrinsic neutron sensitivity, instead of mixtures of powder and neutron converters, (e) fast luminescence for 2D OSL dosimetry using laser scanning.

and, for that reason, may not be useable or practical for the intended application. Second, other needs may arise from yet-to-be-envisioned TL applications. For example, recently a composite TLD consisting of a thin layer grown (usually with the liquid-phase-epitaxy) onto a thick crystal substrate, following the example of a phoswich scintillator, was proposed to achieve a more differentiated TL response for different types of radiation, beta- or alpha-rays (Witkiewicz-Lukaszek et al., 2020). In this case, thin films with dosimetric properties must be developed.

2.2.2. OSL

In the case of OSL, an argument can be made that there is a dearth of OSL materials, which would justify at least a commercial interest in developing new ones.

Al_2O_3:C remains almost an ideal material for OSL dosimetry with high sensitivity, single TL peak and low concentration of shallow traps. The dosimetric properties of Al_2O_3:C are well controlled during production, but the material is currently available commercially only as part of an entire dosimetry system. As in the case of TL, one disadvantage is its effective atomic number ($Z_{eff} = 11.3$), which demands the use of correction factors for dosimetry of low-energy X-rays (Yukihara et al., 2009; Al-Senan and Hatab, 2011; Scarboro et al., 2015). Al_2O_3:C,Mg, although developed for three-dimensional memory storage and fluorescent track detection (Akselrod and Kouwenberg, 2018), has also high TL and OSL sensitivities. The disadvantage is a higher concentration of shallow traps than Al_2O_3:C.

BeO shows excellent performance in OSL dosimetry. Since BeO is a commercial product used in the electronics industry, it is readily available and inexpensive; on the other hand, it not produced specifically for dosimetry and, therefore, the dosimetric properties are not controlled at the production process. BeO became more widely used in OSL dosimetry after its "rediscovery" in the late 1990s (Bulur and Göksu, 1998) and its implementation in a commercial dosimetry system sometime later (Sommer et al., 2011) – see (Yukihara, 2020) and references therein. The OSL signal seems to be associated with light-sensitive traps the TL signal from which overlaps with the TL peak at ~310 °C, which is not strongly affected by light exposure (Yukihara, 2020). BeO, with an effective atomic number of 7.2, is more tissue equivalent than Al_2O_3.

Higher sensitivity. As in the case of TL, the range of sensitivities from commercial OSLDs is also sufficient for environmental and personal dosimetry. Nevertheless, even greater sensitivity is required in dose mapping, because of the need to produce uniform dosimetric films consisting of powder of small grain sizes (Li et al., 2014; Ahmed et al., 2017; Sądel et al., 2020b). More sensitive dosimetric materials could either lower the detection dose limits or open new options when it comes to film and reader development. Materials with higher sensitivity would also allow particles to be embedded in polymers for tissue-equivalent 2D or even 3D dosimetry (Nyemann et al., 2020).

Improved precision. Although annealing can be avoided in OSL dosimetry, precision is still limited to sensitivity changes caused by the dose history of the detector, the presence of supralinearity or saturation, the photon-energy dependence, and other influencing factors. Both Al_2O_3:C and BeO show sensitivity changes as a function or irradiation/bleaching cycles (Yukihara et al., 2005, 2016). An OSL material with no sensitivity change with re-use, if feasible, could greatly simplify the calibration procedure and improve the precision and accuracy of the technique. Since such sensitivity changes are typically related to the elimination of competing processes during irradiation and/or readout, which also results in supralinearity behavior (Chen and McKeever, 1997), an OSL material with linear behavior and saturation at very high doses may show reduced sensitivity changes.

Higher saturation doses. OSL dosimetry using Al_2O_3:C and BeO is limited to doses <100 Gy, since both materials are saturated for doses above that. Therefore, the need for materials that saturate at higher doses is also more urgent in the case of OSL, in addition to the already discussed benefits related to improved precision.

Reduced ionization quenching. As in the case of TL, materials with reduced ionization quenching have the potential to improve the accuracy in ion beam dosimetry due to the reduced need for LET-dependent correction factors. It was recently demonstrated that MgB_4O_7:Ce,Li can provide quenching-free dosimetry for proton beams due to reduced ionization quenching (Yukihara et al., 2022a), but this material is not yet commercially available. Even in the case of MgB_4O_7:Ce,Li a strong quenching for carbon ions used in radiation therapy is still observed, although to a lesser degree than Al_2O_3:C (Yukihara et al., 2022a).

Multiple OSL signals. As in the case of TL, multiple OSL signals have been proposed for neutron-gamma discrimination (Mittani et al., 2007) and for LET measurements in proton beams (Sawakuchi et al., 2010). Nevertheless, so far this has been restricted to the UV and blue emission bands or to the shape of the OSL curves in Al_2O_3:C (Flint et al., 2016; Christensen et al., 2022). Similar effects have not yet been observed in

other OSL materials. The discovery of other dosimetric materials with multiple OSL signals with different LET or photon energy responses could help improve the dosimetry in complex fields.

Neutron sensitivity. None of the commercially used OSL materials (Al_2O_3:C and BeO) are sensitive to neutrons. A neutron-sensitive OSL dosimeter was developed by coating Al_2O_3:C powder with $^6Li_2CO_3$, which works as a neutron converter (Yukihara et al., 2008). Nevertheless, the particles produced during the neutron capture reaction with ^6Li need to reach the Al_2O_3:C grains to produce an OSL signal and, therefore, there is a loss in efficiency in this process (Mittani et al., 2007). A material with intrinsic neutron sensitivity, for example containing Li or B in its structure, such as $Li_2B_4O_7$ or MgB_4O_7, which can be enriched with ^6Li or ^{10}B, can potentially provide better neutron/gamma discrimination (Yukihara et al., 2017; Ozdemir et al., 2018). Fig. 2d illustrates the situation in which the neutron converter is outside the detector grain, and one in which it is intrinsic part of the host material; in the first case, not all the energy from the products of the neutron capture reaction will reach the detector. Although an OSL material with intrinsic neutron sensitivity would provide a competitive advantage in comparison with the existing solution of combining an OSL material with an external neutron converter, the neutron capture reactions with ^6Li and ^{10}B are still dominated by thermal neutrons, decreasing with increasing neutron energies. This means that such OSL material must be used in albedo dosimeters, which rely on the detection of low energy neutrons moderated by the person's body and backscattered towards the detector and, therefore, are strongly dependent on the neutron energy and spectrum (ICRU, 2001).

Faster luminescence lifetimes. For applications in two dimensional dosimetry (dose imaging) both Al_2O_3:C and BeO show luminescence centers that are too slow for laser scanning readout, which is the standard readout technology used in image plates (Leblans et al., 2011). This leads to a phenomenon called pixel-bleeding, which occurs when the laser scans the film faster than the characteristic decay lifetime of the luminescence centers, requiring corrections which can introduce noise to the 2D dose maps (Yukihara and Ahmed, 2015). Therefore, OSL materials with faster luminescence centers are sought for 2D dosimetry (Shrestha et al., 2020a). There is also an interest in OSL materials for three-dimensional dosimetry (Nyemann et al., 2020). Fig. 2e illustrates the concept of 2D dosimetry using OSL films (Ahmed et al., 2014).

As in the case of TL, one must keep in mind that the complete set of requirements for any given application must be taken into account, and that other needs for not-yet-envisioned applications may arise.

3. Strategies for new material development: design rules and their limitations

3.1. The challenges in developing new materials

An overview of the literature reveals a wide variety of materials that have been investigated for their TL/OSL properties and potential application in dosimetry (see Table 2). Nevertheless, few of them reached the status of a commercial material, being produced in large quantities and used in a commercial system. Why is this? The answer lies in the many challenges in producing a working TL/OSL material, as reviewed here.

The challenge in developing new TL/OSL materials derives from the fact that the luminescence and dosimetric properties result from an interplay between host and defects introduced intentionally (and sometimes unintentionally) by doping and by material synthesis, as well as the complex interaction between defects, and the competition between trapping and recombination processes (Townsend et al., 2021). Such complexity has led to the pessimistic statement that "there is no obvious route to optimizing so many parameters, except by trial and error" (Townsend et al., 2021). Although such a statement is true, we believe the number of parameters to be investigated and optimized can be reduced by careful consideration of the fundamentals of dosimetry

Table 2
Examples of synthetic compounds with TL/OSL properties reported in the literature, including effective atomic number, and dopants investigated. Neither the list of hosts or of dopants is exhaustive and, in lieu of a full literature survey, only one key or recent reference is provided for each compound. Recipes for many of the hosts listed here can be found in Yen and Weber (2004).

Compound family	Compound	Z_{eff} (host)	Examples of dopants/co-dopants investigated	Ref.
Halides	CaF_2	16.9	Li, Mn, Al Ce, Tb, Gd, Dy, Eu, Tm, Nd	McKeever et al. (1995)
	KCl	18.1	Cu	Bandyopadhyay et al. (1999)
	NaCl	15.3	Ca,Cu,P, Mg	Gaikwadl et al. (2016)
	KBr	31.5	Eu	Pedroza-Montero et al. (2000)
	LiF	8.3	Mg, Ti, Cu, P, Si	McKeever et al. (1995)
	NaF	9.6	Mg, Cu, P	Gaikwad et al. (2016b)
	$NaMgF_3$	10.4	Ce, Mn	Le Masson et al. (2002)
	$KMgF_3$	14.7	Ce, Eu	Le Masson et al. (2002)
	$BaMgF_3$	48.2	Eu	Quilty et al. (2008)
	$LiKYF_5$	31.3	Pr	Coeck et al. (2002)
	KYF_4	30.7	Ce, Tb, Dy, Tm	Kui et al. (2006)
	K_2YF_5	28.8	Ce, Tb, Dy, Pr, Tm	Marcazzo et al. (2011)
	$LiCaAlF_6$	14.1	Eu,Y	Dhabekar et al. (2017)
	RbMgF3	30.2	Eu	Dotzler et al. (2009)
	RbBr	36.1	Tb	Manimozhi et al. (2007)
	$(NH_4)_2BeF_4$	9.4	Tl	Le Masson et al. (2004)
Aluminates	$MgAl_2O_4$	11.2	C, Tb	Pan et al. (2021)
	$Y_3Al_5O_{12}$	32.3	Ce, Pr, Nd, Sm, Eu, Gd, Tb, Dy, Ho, Er, Tm, Yb	Milliken et al. (2012)
	$CaAl_2O_4$	14.8	Eu, Nd, Dy, Tm	Zhang et al. (2014)
	$LaAlO_2$	49.4		Shivaramu et al. (2018)
	$YAlO_3$	32.3	Ni, Dy, Mn, Yb, Ce	Dhadade et al. (2016)
	$ZnAl_2O_4$	22.4	Tb	Menon et al. (2008)
	$LiAlO_2$	10.7		Holston et al. (2015a)
	$Li_2Al_2O_4$	10.7	Tb	Mittani et al. (2008)
	$SrAl_2O_4$	29.3	R, Ln (R = Li, Na, K) (Ln = Eu, Dy, Nd)	Chernov et al. (2019)
Borates	CaB_4O_7	13.2	Ce, Mn, Cu, Dy, Pb	Hemam et al. (2018)
	CaB_6O_{10}	12.3	Ce, Li, Cl	Oliveira and Baffa (2017)
	MgB_4O_7	8.5	Dy, Tm, Ce, Co	Yukihara et al. (2017)
	$Li_2B_4O_7$	7.3	Mn, Cu	McKeever et al. (1995)
	LiB_3O_5	7.3	Cu	Kananen et al. (2018)
	SrB_4O_7	27.8	Eu, Dy	Palan et al. (2016a)
Binary oxides	Al_2O_3	11.3		

(continued on next page)

Table 2 (*continued*)

Compound family	Compound	Z_{eff} (host)	Examples of dopants/co-dopants investigated	Ref.
			C, Mg, Si, Ti, Cu, P	Akselrod et al. (1998)
	Gd_2O_3	60.9	Eu	Yeh and Su (1996)
	La_2O_3	54.0	Dy, Eu	Orante-Barrón et al. (2010)
	BeO	7.2	Na, Ce, Ln	Bulur and Göksu (1998)
	MgO	10.8	Li, Ln	Oliveira et al. (2019)
	TiO_2	18.9		Cernea et al. (2011)
	SiO_2	11.7	Ce, Cu, Ag	Okada et al. (2016)
	Y_2O_3	30.6	Bi	Jacobsohn et al. (2008)
	ZnO	28.1	Eu, Er	Rivera et al. (2007)
	ZrO_2	26.6	Mg, Ca, Y, Ti, Nb, W, Ce, Sm, Eu, Gd, Tb, Dy, Er	Nakauchi et al. (2016)
Gallates	$MgGa_2O_4$	26.7	Mn	Luchechko et al. (2018)
Phosphates	$NaLi_2PO_4$	10.5	Ce	Sahare et al. (2016)
	$LiMgPO_4$	11.4	B, Tb, Tm, Er	Sas-Bieniarz et al. (2020)
	$KMgPO_4$	14.4	Tb	Palan et al. (2016d)
	$KCaPO_4$	16.4	Ce	Palan et al. (2016f)
	$KSrPO_4$	29.0	Eu	Palan et al. (2016c)
	$LiCaPO_4$	15.4	Ce	Palan et al. (2016f)
	$LiSrPO_4$	30.1	Eu	Palan et al. (2016g)
	Li_3PO_4	10.9	Cu, Tb	Palan et al. (2016b)
	$Li_2BaP_4O_7$	42.5	Eu, Cu	Hatwar et al. (2014)
Silicates	Y_2SiO_5	63.8	Ce	Twardak et al. (2014a)
	Mg_2SiO_4	11.0	Tb	Yoshimura and Yukihara (2006)
	Y_2SiO_5	33.6	Ce	Hazelton et al. (2010)
	$GdSiO_5$	53.8	Ce	Hazelton et al. (2010)
	$LuSiO_5$	60.4	Ce	Hazelton et al. (2010)
	$CaSiO_3$	15.6	Ce	Palan et al. (2016e)
	$Lu_{(1-x)}Y_xSiO_5$	60.4–63.8	Ce	Jensen et al. (2022)
Fluorosilicate	Na_2SiF_6	10.7	Cu, P	Barve et al. (2015)
	$(NH_4)_2SiF_6$	10.4	Tl	Le Masson et al. (2004)
Sulfates	$CaSO_4$	15.6	Dy, Tm	McKeever et al. (1995)
	$BaSO_4$	47.0	Eu, P	Patle et al. (2015a)
	$K_3Na(SO_4)_2$	15.4	Cu, Mg	Gaikwad et al. (2016a)
	$K_2Ca_2(SO_4)_3$	15.8	Eu	Kumar et al. (2015)
	$MgSO_4$	12.2	Ce	Le Masson et al. (2001)
	$SrSO_4$	30.3	Eu	Patle et al. (2015b)
Sulfide	CaS	18.5	Eu, Sm	Liu et al. (2008b)
	SrS	34.6	Eu, Ce, Sm, B	Liu et al. (2008a)
	MgS	14.6	Ce, Eu, Sm	

Table 2 (*continued*)

Compound family	Compound	Z_{eff} (host)	Examples of dopants/co-dopants investigated	Ref.
				Missous et al. (1992)
Halosulfates	$KCaSO_4Cl$	16.6	Ce, Dy, Mn, Pb	Thakre et al. (2012)

and luminescence, coupled with knowledge of the relevant literature.

In the quest for better OSL/TL materials it is crucial to have a good understanding of the various processes involved in the production of the luminescence. The energy of the radiation field is converted by the material into TL or OSL in several, distinct steps (Bos, 2001b). The first step is the absorption of the ionizing radiation and the creation of electron-hole pairs. The next step is the thermalization and trapping of the charge carriers. Only a small fraction of the charge carriers are captured in the traps, which can then be stimulated by heat (TL) or light (OSL), or can act as recombination sites for the released charges. During stimulation, a certain fraction of the captured charge carriers will be released and transported to a luminescence center. If the traps and recombination sites are well separated, there is the inherent problem that other mechanisms may interfere or compete with the desired recombination process (known as competition). Finally the de-excitation of the luminescence center with the emission of a photon occurs with an efficiency that can be reduced if non-radiative pathways exist. Among these different steps, trapping appears to be the least efficient (Bos, 2001b). This means that from the viewpoint of efficiency, traps may deserve more attention than luminescence centers.

From this brief overview, we see that the TL and OSL processes necessarily require two types of defects to exist: at least one type of trapping center and at least one type of recombination/luminescence center. One must, therefore, optimize their concentrations in the crystals, avoiding the high concentrations which can lead to tunneling, and therefore to anomalous fading, or to concentration quenching and its associated reduction in luminescence efficiency, yet a high enough concentration to ensure a high enough signal and a close enough spatial association between the traps and the recombination/luminescence centers to discourage competing processes.

An illustration of the difficulty to discover the nature of the trapping center is seen in the research on the strontium aluminates. $SrAl_2O_4:Eu^{2+}$, Dy^{3+} is a well-known storage phosphor with a very long afterglow (Matsuzawa et al., 1996). It is known that the trapping capacity significantly increases upon Dy^{3+} addition. So it is tempting to identify the trivalent co-dopant as a trap. Until recently, there was no hard evidence to confirm or reject a valence state change for Dy^{3+}. By combining laser excitation and X-ray spectroscopy, Joos et al. (2020) showed that exposure to violet light induces charging by oxidation of Eu^{2+} while Dy^{3+} is simultaneously reduced. Oppositely, detrapping of electrons from Dy^{2+} ($Dy^{2+} \rightarrow Dy^{3+} + e^-$) occurs by infrared illumination yielding optically stimulated luminescence. This confirms the model where Dy^{3+} acts as the main electron trap.

Complications arise when more than one trapping center or recombination center exist, which is often the case in many materials. These defects can be introduced by contaminants in the starting reagents or can be intrinsic defects introduced by the synthesis procedure or by the need to equilibrate charge imbalances due to doping. For example, the introduction of a divalent ion in a trivalent site may favor the formation of anion vacancies to compensate for the charge imbalance (Zhydachevskii et al., 2007). These additional defects may compete for the capture of charges or recombination in the crystal, potentially decreasing the TL/OSL sensitivity.

It is also important to mention the role of thermal treatment (annealing) in establishing or re-establishing the TL/OSL properties of some materials. Annealing not only can promote the recombination of

the trapped charges created by exposure to radiation, but can also help establish an equilibrium between isolated and aggregated defects in the material, thereby improving their properties (Horowitz et al., 2019). If the temperature is too high, annealing can permanently destroy the defects responsible for the TL signal (Tang, 2000).

Further, it should be realized that, in most TL/OSL dosimetry materials, trapping and recombination centers are not independent and decoupled. In many cases, they form clusters of dopants and possible intrinsic effects. These clusters may be difficult to engineer but nevertheless may be critical in the design of new, more efficient luminescence dosimeters (Townsend et al., 2021).

3.2. Possible strategies and limitations

So there is a need for new materials with tailored properties for specific applications. The question is whether there is a basic research strategy that can be applied in the quest to new TL/OSL materials. Can they be designed? Are there design rules? Is there a guide in what areas to search or not to search?

3.2.1. Basic considerations

Although different strategies can be adopted, there are some common aspects that are worth considering beforehand.

Host. As discussed in Section 2.1.3, the host is primarily responsible for the photon energy response (see Section 2.1.3). Although a wide variety of hosts have been investigated (Table 2), most commercial dosimetric materials do not exceed an effective atomic number of 16 (Table 1). The choice of host also determines the type of ions that are more likely to be incorporated as dopants, based for example on ionic radius and valences. Intrinsic defects typical of the host may also be responsible for trapping or recombination centers.

Dopants as recombination/luminescence centers. It is important to introduce dopants that can act as recombination/luminescence centers, providing an efficient radiative recombination pathway for the charges. It is also important that the emission wavelengths match the responsivity of the detection systems and, in the case of OSL, that the emission does not overlap the wavelength of the stimulation light. In fact, it is preferable that the OSL emission occurs at wavelengths shorter than the stimulation wavelength, because when measuring at wavelengths longer than the stimulation light, a fluorescence background from the material or other sources can obscure the OSL signal, particularly at low doses (Yukihara et al., 2022b).

The luminescence centers are typically easier to identify and, therefore, to control. This is because the light emitted can serve as a signature of the corresponding defect. For example, the 4f-4f transitions from some lanthanide (Ln) ions (e.g. Pr^{3+}, Sm^{3+}, Eu^{3+}, Gd^{3+}, Tb^{3+}, Dy^{3+} and Tm^{3+}) are characterized by a series of narrow lines that are not strongly affected by the crystalline field (Blasse and Grabmaier, 1994; Yen et al., 2007), although broad 5d-4f transitions can also be observed in some cases (e.g. Pr^{3+}, Nd^{3+}), depending on the host matrix (Blasse and Grabmaier, 1994). As a result, these particular lanthanides can be easily identified. For other lanthanides characterized by broad 5d-4f emission, the emission wavelengths depend strongly on the host material (e.g., Ce^{3+}, Eu^{2+}); in such cases, the emission wavelength is well known for various compounds (Dorenbos, 2000b, 2003), or can sometimes be inferred based on similar compounds and considering the differences in the crystalline environment (Dorenbos, 2000a). Photoluminescence emission and excitation data can help identify the luminescence centers, if the photoluminescence and TL/OSL emission bands are shown to be the same. For example, photoluminescence spectra from transition metals (e.g. Mn, Cr, Ti, Ni) can be used in conjunction with the Tanabe-Sugano diagrams to try to identify the luminescence centers and crystal field effects surrounding the ions (McKeever et al., 1986; Henderson and Imbusch, 1989; Blasse and Grabmaier, 1994).

The incorporation of luminescence centers in the host can also be tested by measuring the radioluminescence spectrum. This does not imply, however, that the same defects act as luminescence centers during the TL/OSL processes. This must be confirmed by measuring the TL/OSL emission spectra.

Fig. 3, for example, shows the TL emission spectra for $CaSO_4$ systematically doped with various lanthanides. The emission lines from Pr^{3+}, Sm^{3+}, Eu^{3+}, Gd^{3+}, Tb^{3+}, Dy^{3+} and Tm^{3+} are clearly seen in the respectively doped compounds. In addition, one can also see Eu^{2+} broad-band emission at 384 nm in the Eu-doped compound (Fig. 3e). Such data are useful to confirm or reveal the dominant luminescence centers involved in the recombination process.

Color centers as recombination/luminescence centers. TL or OSL emission from some materials can be identified as originating from color centers, such as *F* and F^+-centers in the TL and OSL of Al_2O_3:C (Akselrod et al., 1990; Markey et al., 1995), or a variety of *F*-center-related centers in the TL of Mg,Cu,P-doped LiF, especially at high doses (McKeever et al., 1995). Impurity-perturbed color-center emission in these materials can also be identified (McKeever et al., 1995; Sanyal and Akselrod, 2005).

Co-dopants as trapping centers. Compared to luminescence centers, trapping centers (traps) are more difficult to identify and, therefore, to control, because their involvement in TL and OSL is indirectly detected through the luminescence. They can be identified, although not unequivocally, if a dopant clearly introduces a new TL peak. Unambiguous identification, however, is only possible in some cases, and requires time-consuming correlative studies in which the TL/OSL signals are compared with electron paramagnetic resonance (EPR) signals after various doses or treatments (thermal or optical). Moreover, it is also often the case that a dopant changes not only one TL peak but several, suggesting the unintentional introduction of other intrinsic defects, contaminants, or multiple defect combinations that shape the TL curve (Townsend et al., 2021). Models for TL/OSL trapping centers exist only for a few materials, among them quartz (Martini and Fasoli, 2019) and LiF:Mg,Ti (Horowitz et al., 2019; McKeever, 2022); even in those cases, sometimes competing models exist.

The introduction of efficient trapping centers is likely the most serendipitous aspect here, varying significantly with conditions such as synthesis method, annealing, other co-dopants, etc. As we will see in Section 3.2.4, the Dorenbos model (Dorenbos, 2020) provides some guidance on the choice of lanthanides as co-dopants; the location of the lanthanide energy levels within the bandgap can indicate the lanthanides that are most likely to act as electron or hole traps. Besides that, one must often rely on the literature or attempt new dopant combinations serendipitously.

Other co-dopants. Other co-dopants have been shown to increase considerably the RL, TL or OSL in some compounds. As an example, Li-co-doping is known to improve the luminescence in lanthanide-doped MgO (Orante-Barrón et al., 2011), MgB_4O_7 (Yukihara et al., 2014b) and $Y_3Al_5O_{12}$ (Milliken et al., 2012). In the case of the Mg-based compounds, it is speculated that Li^+ substituting for Mg^{2+} serves as charge compensation for the Ln^{3+} substituting for Mg^{2+} (Orante-Barrón et al., 2011). Na and K may have similar roles in other hosts. In some samples co-doped with two different lanthanides, it has also been observed that the compounds with two dopants have higher signal than singly-doped compounds (Bastani et al., 2019), but more in-depth studies are required to elucidate the mechanism responsible.

Synthesis reagents and methods. The synthesis reagents and methods affect the resultant TL/OSL due to various factors, including trace contamination from the reagents or preparation procedure, the degree of disorder, intrinsic defects introduced by the synthesis or post-synthesis annealing, the distribution of dopants in the matrix, and so on. In MgB_4O_7:Ce,Li, for example, it has been shown that one can eliminate a recombination route competing with the Ce-ions and improve the sensitivity of the material by reducing Mn contamination during synthesis (Gustafson et al., 2019).

Although not always the case, the knowledge gained with one

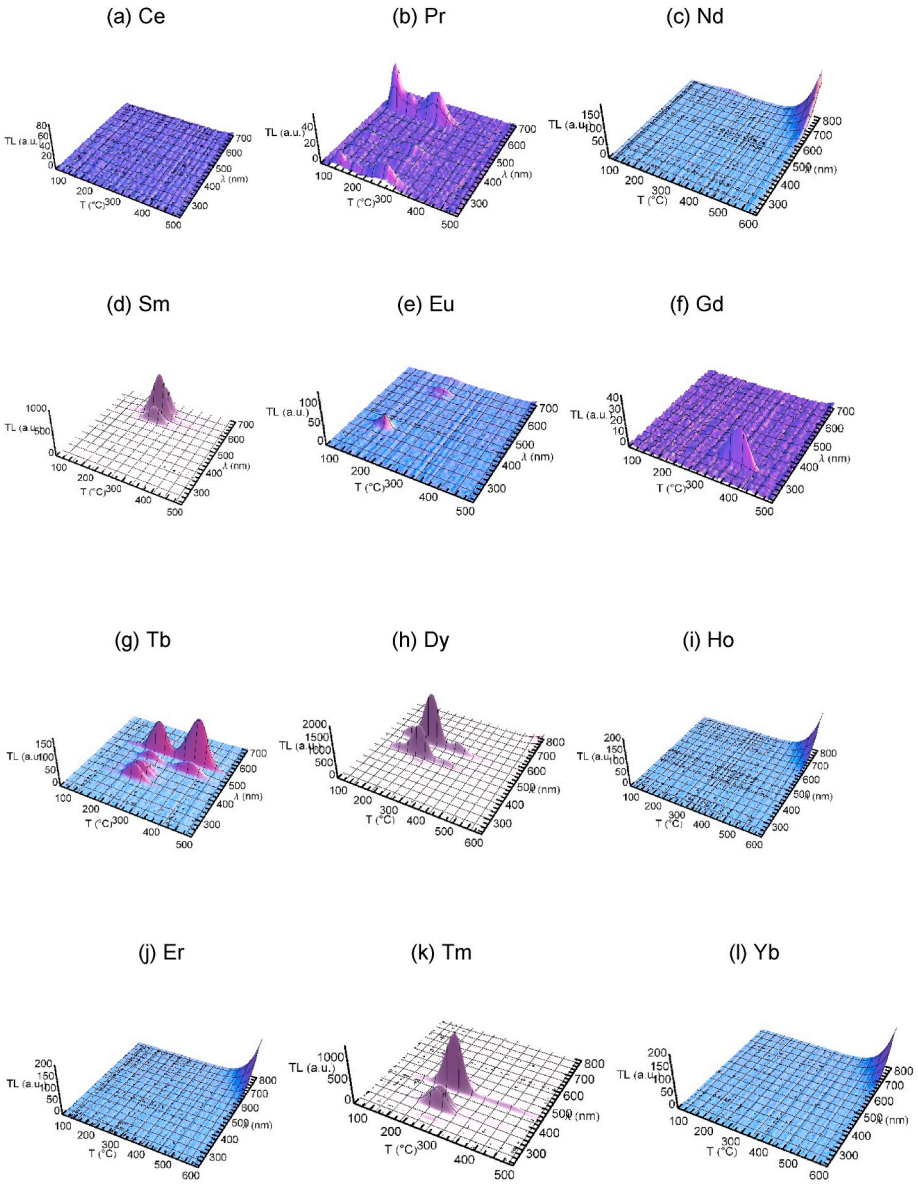

Fig. 3. Example of TL emission spectra of $CaSO_4$ doped with various lanthanides, showing some of the characteristic emissions of Ln^{2+} (e.g. Eu) and Ln^{3+} (e.g. Pr, Sm, Eu, Gd, Tb, Du, and Tm) (Bastani et al., 2019).

synthesis method may be translated to another method. Using MgB_4O_7:Ce,Li as an example, it has been shown that MgB_4O_7:Ce,Li glass-ceramics could be produced with properties very similar to those prepared by solution combustion synthesis (Kitagawa et al., 2021).

3.2.2. *Modification of existing luminescent materials*

Based on existing materials, researchers have attempted to improve the luminescence and dosimetry properties by different approaches. One possibility is to start with materials found in the environment. These natural materials can be low-cost and available in reasonably large quantities. Examples are CaF_2 (Guimarães and Okuno, 2003), Brazilian topaz (Sardar et al., 2013) and Alexandrite (Nunes et al., 2020); natural CaF_2 has been used routinely for dosimetry for decades at the University of São Paulo (Guimarães and Okuno, 2003; Umisedo et al., 2020). The disadvantage is that the material composition is not exactly known and not controllable. Nevertheless, it is possible that the study of natural materials can be a starting point for the development of synthetic versions with more controlled properties.

In the same way that the development of LiF:Mg,Cu,P, LiF:Mg,Cu,Na, Si and LiF:Mg,Cu,Si was motivated by the need to improve the sensitivity of LiF:Mg,Ti, studies involving new synthesis procedures, new dopants or dopant combinations, or new thermal treatments may lead to improvements over the materials already reported in the literature.

For example, LiF:Mg,Cu,P was introduced as a phosphor with sensitivity higher than that of LiF:Mg,Ti, and with a different TL curve (Nakajima et al., 1978). The disadvantage is the loss in sensitivity if heated above 240 °C and, without that, an increase in the residual signal with dose due to incomplete erasure of the so-called peak 5 (McKeever et al., 1995). By replacing P with Si and changing the preparation and annealing procedures, it has been shown that LiF:Mg,Cu,Si can be heated to 300 °C and the sensitivity of peaks 1–4 can be recovered by annealing to 240 °C (Lee et al., 2006). This approach increased the sensitivity while maintaining advantages such as the Z_{eff} (Lee et al., 2008).

Improving the dosimetric properties does not necessarily require the introduction of new dopant species. In some cases, it may be possible to obtain a material with very different properties only by changing the amounts of the existing dopants and preparation conditions. LiF can be

used again as an example. Through systematic investigations of the influence of Mg and Ti contents on the relative efficiency to heavy charged particles, it was possible to obtain detectors with the increased high-LET response (Bilski et al., 1999, 2004).

Dopants can be used as luminescence centers having emission that is a better match to the detection system's sensitivity or the intended technique. For example, MgB_4O_7:Dy is a well-known TL dosimeter (McKeever et al., 1995) also developed for particle temperature sensing (Doull et al., 2014). For OSL applications, however, an emission with wavelength shorter than green/blue stimulation is desired, which led to MgB_4O_7:Ce^{3+}, since Ce^{3+} has an emission in the UV in the MgB_4O_7 host (Gustafson et al., 2019). Co-dopants can favor the introduction of specific defects and aggregations, as discussed in Section 3.2.1.

Attempts have been made to improve specific properties by controlling the size of the particles. For example, phosphors in nanocrystalline form with average grain size of ~30 nm (nanophosphors) were shown to exhibit high radiation resistance and an increased saturation dose, raising the upper limit of the useful dose range, but with lower overall sensitivity (Kortov, 2010; Salah et al., 2011). It has also been suggested that core-shell nanoparticles containing a metal nanoparticle core can enhance the OSL stimulation rate in the shell material (Guidelli et al., 2015).

It is well-known that the synthesis method has a great impact on the TL and OSL properties. It is therefore not surprising that research into the synthesis itself has been used to improve the properties. Yukihara et al. (2013) explored the Solution Combustion Synthesis (SCS) method. ZnO samples synthesized by co-precipitation and sol-gel methods and subject to different heat treatments were studied (Soares et al., 2017; Guckan et al., 2020). The effect of annealing and fuel type on the TL properties of $Li_2B_4O_7$ synthesized by Solution Combustion Synthesis were also reported (Doull et al., 2013; Wang et al., 2013).

Another approach has been to investigate compounds known for their scintillation or radioluminescence properties. In this way, we start with already pre-selected materials, which are known to exhibit a high luminescence yield. What remains to be done is to generate appropriate trapping sites in the host material. Normally, the trapping of charge carriers is an unwanted effect in scintillators. Nevertheless, through changing dopant concentrations, co-doping, or changing material preparation conditions, this may be achieved. Examples of potential dosimetric materials developed using well-known scintillators as a host include: TL and OSL detectors based on Mn-doped yttrium perovskites (Zhydachevskii et al., 2010, 2016), OSL of Ce-doped orthosilicates (Hazelton et al., 2010; Twardak et al., 2014b; Jensen et al., 2022), and IR-induced OSL of Ce-doped mixed Gd/Ga garnets (Bilski et al., 2021). A shortcoming of this approach is that typical scintillating materials, such as those mentioned, possess high effective atomic numbers (see Section 2.1.2).

3.2.3. *Systematic search for host/dopant combinations*

There have been a few attempts to systematically survey a broad range of host/dopant combinations with the goal of developing new TL/OSL materials or to elucidate their luminescence properties. Examples are work on CaF_2 (Merz and Pershan, 1967b, a; Awata et al., 1999), $CaSO_4$ (Nambi et al., 1974; Bastani et al., 2019), Mg_2SiO_4 (Zhao et al., 2019), and BeO (Altunal et al., 2021). Such investigations are time-consuming and laborious.

The advantage of using a systematic approach, however, is that it provides a better comparison between the samples by allowing more control of the synthesis method, reagents and steps, as well as of the measurement equipment and procedures. In such studies the probability of identifying the effect of a particular dopant is higher.

$CaSO_4$ has been extensively studied for its TL/OSL properties for decades. An example of a systematic study, Medlin (1961) investigated the TL for $CaSO_4$ precipitated with several dopants chosen based on the analysis of natural calcite (Mn^{2+}, Zn^{2+}, Sb^{2+}, Pb^{2+} and Cd^{2+}) at different concentrations. The determination of the concentration curve, as exemplified in this study, is particularly important, because at high dopant concentrations the sensitivity typically falls due to concentration quenching.

A systematic investigation on the TL of $CaSO_4$ doped with various lanthanides was also reported (Nambi et al., 1974). In addition to providing typical emission spectra for the various combinations and identifying the most efficient activators of the TL (Dy and Tm), the study also indicated that the TL curves were similar, regardless of the dopants. This suggests that intrinsic defects are responsible for the trapping centers, whereas the lanthanides act as luminescence centers.

Although the study above represents a step in the right direction, there is a loss of information when the TL emission spectra and the TL curves are presented separately as in Nambi et al. (1974). New insights can be obtained if the information is combined and presented together in contour plots or 3D graphs of intensity versus wavelength and temperature.

As an example, Fig. 3 shows the results from a study similar to Nambi et al. (1974) on the TL emission spectra of various lanthanide-doped $CaSO_4$ samples, but with the data presented in the form of 3D graphs (Bastani et al., 2019). In most cases, the data confirm the observations from Nambi et al., i.e. the TL emission is characteristic of the trivalent lanthanide (Ln^{3+}) introduced during the synthesis. In the case of Eu, however, the TL emission spectrum shows both Eu^{2+} and Eu^{3+} emissions, but the TL peaks associated with each of these emissions are different (Fig. 3e): for the Eu^{2+} emission at 384 nm, the TL peak occurs at ~150 °C, whereas for the Eu^{3+} emission lines at 591 nm, 619 nm, 658 nm, the TL peak occurs at ~225 °C. These results indicate the possible presence of both electrons and hole traps, which leads to the recombination of the released electrons and holes through $Eu^{3+} + e^- \rightarrow (Eu^{2+})^*$ and $Eu^{2+} + h^+ \rightarrow (Eu^{3+})^*$, where Eu^{2+} or Eu^{3+} luminescence is observed upon relaxation of the excited $(Eu^{2+})^*$ and $(Eu^{3+})^*$ defects. Based on that, Bastani et al. (2019) proposed a tentative model for the recombination processes in other lanthanide-doped $CaSO_4$ samples.

A systematic investigation of various host/dopant combinations was also recently carried out (Yukihara et al., 2013). This search was focused on materials that could be produced by solution combustion synthesis, which facilitated the rapid synthesis of various host-dopant combinations. Materials synthesized include ZrO_2, Y_2O_3, $MgAl_2O_4$, $Y_3Al_5O_{12}$, $LaMgB_5O_{10}$, CaO, MgB_4O_7, Al_2O_3, $CaAl_{12}O_{19}$, $Li_2B_4O_7$, $CaAl_2O_4$, MgO, and $LiAlO_2$, with a wide variety of dopants and co-dopants. This study led to the identification of a few compounds with high TL intensity and low light sensitivity for applications in temperature sensing, including $Li_2B_4O_7$:Cu,Ag, MgB_4O_7:Dy,Li and $CaSO_4$:Ce,Tb (Doull et al., 2014; Yukihara et al., 2014a, 2015). Furthermore, it also led to the identification of MgB_4O_7:Ce,Li as a high-sensitivity OSL material with fast luminescence (31.5 ns lifetime), due to Ce^{3+} emission, for applications in 2D OSL dosimetry by laser-scanning readout (Yukihara et al., 2017; Shrestha et al., 2020a), and with lower ionization quenching for applications in proton therapy (Yukihara et al., 2022a). For $Li_2B_4O_7$ the influence of the fuel (urea, glycine, ammonium nitrate) used in the solution combustion on the TL properties was investigated (Doull et al., 2013).

The TL and OSL of BeO was also systematically investigated as a function of lanthanide doping (Altunal et al., 2021). Properties such as the radioluminescence spectra, OSL emission spectra, TL curves and OSL curves were investigated as a function of dopant, co-dopant, and dopant concentration. The study demonstrated changes in both radioluminescence emission spectra and TL curve shapes as a function of the dopants. The authors identified suitable dopant combinations for further development.

The TL emission spectra of Mg_2SiO_4 doped with various lanthanides was investigated (Zhao et al., 2019), which provided a possible interpretation for the shifts in TL peak as a function of the lanthanide ionic radius. These studies should now be followed by more in-depth investigations to take advantage of the knowledge gained to develop materials of practical use.

3.2.4. Model-guided approaches

A fundamentally new research strategy is based on defect and bandgap engineering based on a model as a guide for the development of new materials. Dorenbos – see (Dorenbos, 2019, 2020) and references therein – developed a phenomenological model predicting the absolute location of 4*f* and 5*d* states of lanthanides in different compounds. The model predicts all 4*f* and 5*d* ground state levels of both the divalent and trivalent lanthanides in a compound with only three parameters which can be derived from spectroscopic data. Fig. 4 shows the energy levels calculated, for example, in $Y_3Al_5O_{12}$ (YAG) (Milliken et al., 2012). With those level positions, one can predict the character of the defects. For example: when the divalent lanthanide 4*f* ground state levels are below the conduction band, the corresponding trivalent ions may act as electron traps. On the other hand, trivalent lanthanides may act as recombination centers when they show a large energy gap between the ground state and the top of the valence band. This model provides a guide to potentially useful combinations of host and dopant to be investigated and, even more importantly, indicates combinations that are not likely to work. This knowledge was used to design new dosimetric materials by systematic investigation (Yukihara et al., 2013; Oliveira et al., 2019). Nevertheless, it should be noted that, despite the fact the model is useful in predicting the TL peak temperature and emission wavelengths, it does not predict the emission intensity and, therefore, the sensitivity.

Band gap engineering is a similar technique. Instead of doping the host to introduce energy levels in the band gap (defect engineering), the composition is altered to change the band structure of the host (band gap engineering) (Fasoli et al., 2011). For example in $Y_3Al_{5-x}Ga_xO_{12}$:Ce^{3+},Cr^{3+} (YAGG:Ce^{3+},Cr^{3+}), a persistent phosphor which emits bright green light due to Ce^{3+} 5*d* →4*f* transition, the energy gap between the lowest 5*d* state of Ce^{3+} and the bottom of the conduction band can be decreased by increasing Ga^{3+} substitution (Ueda et al., 2015; Katayama et al., 2017), since the substitution alters the position of the bottom of the conduction band. In a similar way, the top of the valence band can be engineered to control the energy levels of potential hole trapping centers (Luo et al., 2016).

Detailed material-specific models of the TL/OSL processes, such as those proposed for quartz (Martini and Fasoli, 2019) and LiF:Mg,Ti (Horowitz et al., 2019), in which the defects and/or trapping/-recombination pathways are described, may also guide sensitivity improvements in existing materials by identifying opportunities for reducing competing processes. One possibility already discussed in Section 3.2.2 is to eliminate contaminants responsible for alternative recombination pathways, such as Mn in MgB_4O_7:Ce,Li (Gustafson et al., 2019). Annealing may also help eliminate intrinsic defects that act as competitors. Such potential improvements, however, can more easily be identified if a model exists describing the defects and their roles in the TL/OSL processes.

If the trapping and recombination centers are known and their spatial proximity can be inferred, another possibility to reduce competition is by increasing the probability for localized recombination. That may be achieved by producing phosphors in which the trap and the luminescence site are close enough for localized recombination to occur. Fig. 5 illustrates several possibilities for recombination between a trapping center and a recombination center that are closely located, such as tunneling from the ground state or excited state of the trapping center to excited states of the recombination center, in addition to recombination involving the delocalized band.

Localized recombination was shown to be fundamental for the description of the infrared stimulated luminescence in feldspars (Jain et al., 2015) and of the TL in YPO_4:Ce,Ln (Ln = Er, Ho, Nd, Dy) (Dobrowolska et al., 2014). The idea is to engineer a TLD or OSLD material with trapping and recombination centers close enough so that they do not have to undergo delocalized recombination and suffer from competition effects, but instead recombine via excited-state tunneling, resulting in TL or OSL.

Nevertheless, it is important for the trap and the recombination center not to be too close, to avoid ground-state tunneling that can lead to anomalous fading. The wavefunction in the excited state is more extended, so excited state tunneling occurs over greater lattice distances

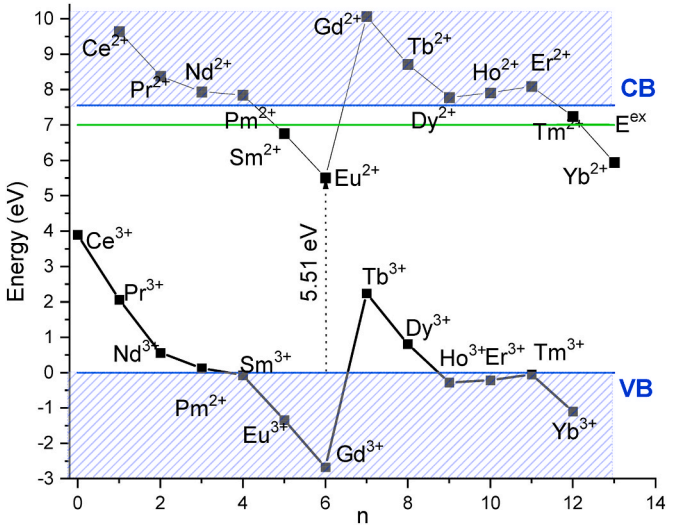

Fig. 4. Energy level scheme of the divalent and trivalent lanthanides in $Y_3Al_5O_{12}$ (YAG), calculated by Milliken et al. (2012). From this energy level scheme it can be predicted that Ce^{3+} and Tb^{3+} can act as deep hole traps and Sm^{2+}, Tm^{2+} and Yb^{2+} as deep electron traps. For more details on how to interpret such a scheme and its relation to the thermoluminescence processes, see Dorenbos and Bos (2008).

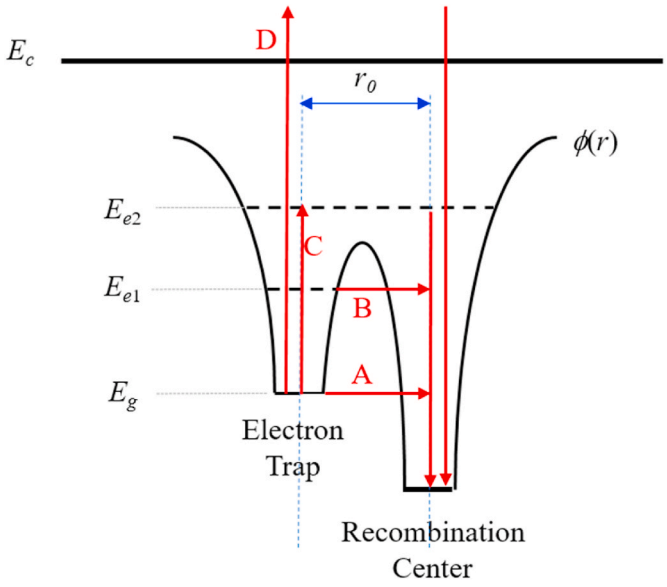

Fig. 5. A schematic potential energy diagram in the vicinity of a trap and a recombination center showing several possible recombination pathways, depending upon the proximity of the trap and center (r_0). If close enough, tunneling directly from a trapped electron in the ground state (E_g) to the recombination center can occur (transition A), leading to anomalous fading. If the electron is excited into an excited state E_{e1}, excited state tunneling can also occur, through a narrower potential barrier and, since the wavefunction is more diffuse, this can occur over greater trap-center (donor-acceptor) distances (transition B). If excited to level shared excited state E_{e2} (transition C) direct, recombination can occur without tunneling. Finally, if enough energy is absorbed, transition D can occur and recombination via the conduction band can take place. Transitions A, B and C are examples of localized recombination and avoid the problem of competition. Transition A, however, leads to anomalous fading.

than ground state tunneling. While fine tuning the defect concentrations may be difficult, a post-irradiation pre-heat to eliminate the nearest-neighbor pairs, and thereby reduce the probability of ground-state tunneling may be feasible, as proposed by Jain and Ankjærgaard (2011) for IR-induced OSL from feldspar.

Close association between trapping and luminescence centers can be inferred from TL/OSL emission spectra. For example, high-resolution 3-D TL emission spectra show that the TL peaks of some phosphors doped with lanthanides shift slightly as the dopant concentration increases. These are indications that the same rare earth affects not just the luminescent site but also the trapping site. Also, small frequency factors are indications of localized recombination. Some examples of both of these were given in Townsend et al. (2021).

The main concept here is that, by forcing localized recombination rather than delocalized recombination, and thereby removing competition, one may be able to increase the material sensitivity and remove the supralinearity in the dose response. Since the dose response to low-LET radiation is connected to the LET-dependence of TL/OSL signal — the final TL/OSL signal after a heavy charged particle irradiation being the convolution of the radial dose distribution and the luminescence response (Horowitz, 1981; Yukihara and McKeever, 2011) — one may also end up improving the LET response, i.e. increasing the LET before ionization quenching sets in (which has to occur eventually because saturation cannot be avoided).

Bos examined two high-sensitivity materials, CaF_2:Cu,Ho and $KMgF_3$:Ce^{3+} and concluded that their high sensitivity is likely related to the existence of localized recombination (Bos, 2001b). It would be useful to examine the myriad of new phosphors mentioned in Table 2 that show promising TL and OSL dosimetry properties, to search for evidence of localized transitions and investigate its influence on the dose- and LET-response characteristics.

4. Common pitfalls

Having discussed the potential strategies to develop useful TL/OSL materials, we turn our attention to some issues that often hinder progress in the field.

4.1. Lack of sensitivity comparisons

As discussed in Section 2.1.1, a sensitivity comparison of a new material against known TL/OSL materials is essential, at least as an approximate estimate to decide if further development for a particular application is worth pursuing.

This comparison is not always straightforward, because it should be performed in optimized conditions for each material in order to allow a proper comparison, e.g. by optimizing the optical filters and detection systems for the emission spectra of each particular material. If this is not possible, then the influence of the experimental conditions on the results must be considered.

For comparison of the sensitivity of a new material, powder form is preferable, since the transparency of pellets and ceramics can influence the results. Even in the case of powder, the signal may not be proportional to the powder weight, depending on the packing of the material during readout. Reducing the amount of powder should decrease this effect, but with an increase in the mass uncertainty.

The materials can also be compared in terms of the minimum detectable dose (MDD). This may be estimated, for given experimental conditions and amount of material, as that dose corresponding to a signal equal to three times the standard deviation of the zero-dose reading (i.e. the response without previous irradiation) (Currie, 1968; Yukihara and McKeever, 2011). Although this quantity depends on the reader and experimental conditions, it gives an idea of the achievable detection limits.

For general dosimetry applications, the comparison should also be performed whenever possible using high energy sources (e.g., ^{137}Cs, ^{60}Co, ^{90}Sr/^{90}Y) because differences in Z_{eff} between the materials may distort the comparison, particularly when using X-rays with energy <100 keV. Therefore, one should also keep in mind the photon energy response when using X-ray sources and comparing samples of different effective atomic numbers.

4.2. Incorrect or aimless analysis of TL/OSL curves

Various analysis methods have been proposed to obtain the kinetic parameters (activation energy, frequency factor, kinetic order) of the TL peaks. The most popular are peak fitting, peak shape method, initial rise method, and the various heating rate methods (McKeever, 1985, 2022; Horowitz and Yossian, 1995; Chen and McKeever, 1997; Sunta, 2015). Various models have been considered for such analyzes, including the first-order and non-first-order models characterized by a kinetic order b (Kitis et al., 1998).

If used correctly and within their limitations, the results of such analyses can be helpful to estimate fading rates of specific TL peaks and compare them to actual fading rates, e.g. to identify anomalous fading. They can also assist in the location of the energy levels within the bandgap (Dorenbos and Bos, 2008) or identify the occurrence of tunneling between defects (Vedda and Fasoli, 2018). Examples where the obtained kinetic parameters correctly predict the fading rate are, nevertheless, rare. In general, the glow peak temperature at the measured heating rate gives more information on the fading then the derived trapping parameters.

Further, it should be said that the results obtained when applying such methods to single TL curves, without validation of the underlying models used in the analyses, are of little value in improving our understanding of the TL process.

Concerning curve fitting, there are three main criticisms that apply when using non-first-order kinetic models:

(a) Non-first-order TL peaks arise in specific conditions, for example when retrapping dominates over other processes (recombination, capture by deep traps). Nevertheless, the rates of retrapping and recombination change with the trap occupancy and during the readout of the TL peaks, which means that the kinetic order, understood as representing a relationship between the retrapping and recombination rates, is not constant with the dose or even within one TL peak (Opanowicz, 1989; Chen and McKeever, 1997). The TL curves in this case can only be described by the solution of rate-equations for the process, and a general-order model with constant b is simply an approximation for the actual process taking place.

(b) Non-first-order behavior also implies interaction between traps during readout (during TL or OSL) and, therefore, the simple superposition principle is not valid. This means that fitting a TL curve with a superposition of non-first-order TL peaks is not physically meaningful (Chen and McKeever, 1997; Chen and Pagonis, 2011).

(c) Broad peaks resembling those predicted by non-first-order kinetics can be observed due to a superposition of first-order TL peaks from closely distributed energy states – see Van den Eeckhout et al. (2013) and McKeever (2022) for recent discussions on this. To distinguish between non-first-order behavior and peaks due to an energy distribution, one must look into the dose dependence of the TL curves. Non-first-order TL peaks should shift to lower temperatures with increasing trap occupancies (McKeever, 1985; Chen and McKeever, 1997; Sunta, 2015).

Fig. 6 illustrates some of the points mentioned above. Fig. 6a shows the behavior of a TL peak for various trap occupancies according to the second-order model, indicating that the TL peak should shift to higher temperatures if the trapping population decreases (e.g. due to pre-

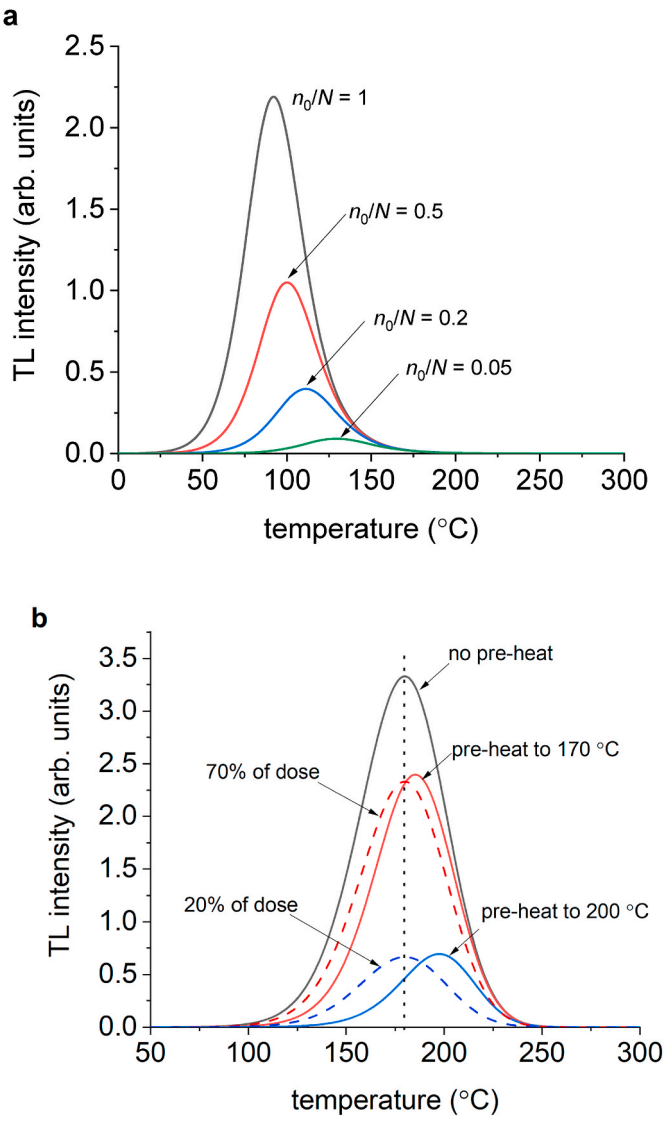

Fig. 6. Comparison between (a) a second-order TL peak ($E = 0.95$ eV, $s = 10^{12}$ s^{-1}) and (b) a first-order TL peak associated with a Gaussian energy distribution ($E_{mean} = 1.2$ eV, FWHM $= 0.05$ eV, $s = 10^{12}$ s^{-1}). In (a), the TL peaks as a function of the dose or pre-heat are the same, since the traps are characterized by a single activation energy and the TL curve intensity and shape are determined by the factor n_0/N, the relative occupancy of the trapping centers (Chen and McKeever, 1997). In (b), the peak position stays constant as the dose increases, but the effect of pre-heating is greater in the low-temperature part of the activation-energy distribution, causing a shift to higher temperatures with increasing pre-heating temperatures. The curves are for a heating rate of 1 °C s^{-1}.

heating) and to lower temperatures if the trapping population increases (by increasing the dose). Fig. 6b, on the other hand, shows the behavior of a TL peak due to a Gaussian distribution of energy in the first-order model. In this case, the peak shifts to higher temperatures with pre-heating, since the traps with lower thermal stability are emptied more by the pre-heating, but remain in the same position if the dose is varied. Such behavior is typically observed in real materials, which points to a distribution of activation energies (or frequency factors) instead of non-first-order behavior.

Furthermore, real TL materials predominantly exhibit first-order behavior, i.e. constant TL peak temperature with dose. This can be related to the presence of many competitive processes, e.g. many recombination pathways or capture by deep traps (Pagonis and Kitis, 2012), or to the possible prevalence of localized recombination (Bos, 2001b). Therefore, there must be evidence supporting the use of non-first-order models for TL analysis. This evidently requires the measurement of TL curves at different doses up to saturation and the study of the TL peak temperatures as a function of dose, and cannot simply be based on the broadness of TL peaks from single TL curves.

Energy distributions can be recovered using methods such as those proposed by Gobrecht and Hofmann (1966) and by Van den Eeckhout et al. (2013), but there are limitations (Coleman and Yukihara, 2018); see also McKeever (2022).

Another issue is related to the influence of thermal quenching. Thermal quenching refers to the reduction in luminescence efficiency as a function of temperature, due, for example, to the increased probability of non-radiative relaxation of the luminescence centers at higher temperatures (McKeever, 1985; Chen and McKeever, 1997). Thermal quenching can distort TL curves and influence other analysis methods. Therefore, before analyzing a TL curve, the curve should be corrected for thermal quenching.

Analyzing OSL curves is perhaps even more difficult, since stimulation at a given wavelength can empty multiple traps simultaneously, and unraveling the individual processes is nontrivial. Fitting the OSL decay curves with a summation of exponentials is rarely helpful, unless it is demonstrated that the components correspond to distinct physical processes (e.g. by identifying components with different thermal stabilities using step-annealing experiments).

4.3. Haphazard investigation

Although haphazard investigation has played a major role in the development of TL materials in the past (McKeever et al., 1995) and it may still lead to the identification of an important TL/OSL material, such studies can rarely be generalized to gain a better understanding of the TL/OSL processes in a class of materials or host. A systematic investigation is, on the other hand, extremely time-consuming and expensive, requiring the synthesis of a large number of samples.

Nevertheless, knowledge of the principles in Section 3.2 can provide a more guided approach to this research, for example, limiting the range of dopants to be investigated. The goal of the research should be to gain general insights on the luminescence processes, through which possibly one or two candidates can be identified for a more-in-depth study and optimization. This systematic approach can possibly be made easier by the adoption of facile synthesis techniques, by which many samples with different dopant combinations can be synthesized for screening and initial characterization. Parallel solution combustion synthesis for combinatorial material studies has been proposed (Luo et al., 2005), but to the best of our knowledge not been used for investigations in TL or OSL. At a later stage, different synthesis processes can be investigated and optimized.

4.4. Lack of correlation with other techniques

Although the TL and OSL emission spectra can assist in the identification of luminescence centers and, therefore, indicate a direction on how to improve the materials, identification of defects responsible for the trapping centers is typically more difficult because the evidence is indirect. The study of TL and OSL curves alone can rarely illuminate the underlying physical processes, unless coupled with systematic investigations with various dopants, as discussed in Section 3.2.3.

To identify the trapping centers, correlative studies between TL/OSL and more defect-specific techniques such as optical absorption, photoluminescence and electron paramagnetic resonance (EPR) are needed. A highly sophisticated technique like X-ray absorption near-edge structure (XANES) can help to identify the change in valence state of the dopant. In a material doped with Eu^{2+} and co-doped with Dy^{3+} one may expect oxidation of Eu^{2+} to Eu^{3+} along with reduction of Dy^{3+} to Dy^{2+}. Such changes in valence change can be observed by measuring XANES spectra (Lastusaari et al., 2015; Joos et al., 2020).

The value of EPR in the identification of radiation-induced defects is well known and its application to TL and OSL processes, although sporadic, can be revealing. Such correlations have helped in the identification of defects involved in the TL process of natural materials such as quartz (McKeever et al., 1985) and topaz (Yukihara et al., 2002). More recently, correlations between EPR and TL have helped to identify the defects involved in the TL peaks in K_2YF_5:Tb^{3+} (Zverev et al., 2011), in $Li_2B_4O_7$:Ag (Brant et al., 2011; Buchanan et al., 2014) and $Li_2B_4O_7$:Cu (Brant et al., 2013). The defects involved in the OSL of $Li_2B_4O_7$:Ag were later identified: EPR/OSL correlative studies indicate that electrons are optically stimulated from Ag^0 center and recombine with holes trapped at Ag^{2+} centers, resulting in UV emission (Kananen et al., 2016). EPR has also been used to identify the defects related to the TL (Holston et al., 2015b) and the OSL (Holston et al., 2015a) in $LiAlO_2$, and to the TL in LiB_3O_5 (Kananen et al., 2018).

5. Conclusions and outlook

In the first part of this review we showed that the need for new TL and OSL materials exists, but is limited to specific applications; any new material must satisfy the requirements for those applications. TL and OSL are already mature dosimetry techniques, being used by various commercial dosimetry systems and employed for individual and area monitoring, as well as medical, research and industrial applications by various laboratories throughout the world. As a result, it is important to identify clearly the problem or application being addressed, while justifying the choices of host and dopants, and comparing the dosimetric properties of the newly proposed materials to well-known and widely available TL/OSL materials.

The second part of this review illustrated several strategies that can be used in these studies, as well as their limitations. Research on new materials for dosimetry applications should: (a) substantially advance the understanding of a physical phenomenon or process, or (b) demonstrate that the material may have advantages compared to existing materials or technologies. These objectives will likely be more efficiently achieved through systematic studies that can be either broad (various hosts and dopant combinations, or one host and various dopant combinations), or specific (one host/dopant investigated under various conditions of annealing, synthesis, dopant concentration). In either case, they should also preferably involve techniques that can help elucidate the underlying mechanisms (TL/OSL with high spectroscopic resolution, optical absorption, photoluminescence, EPR, and others).

Finally, the third part of this review warns against common pitfalls encountered in the literature and suggests alternative approaches. We emphasized in particular the need for: (a) comparing the sensitivity with well-known materials, (b) a more critical use of TL models and curve fitting, for example, by experimentally confirming non-first-order behavior or the existence of a distribution of activation energies, (c) a more guided study that can lead to fundamental and generalizable understanding of the processes, and (d) correlative studies between TL/OSL and other techniques that can provide defect-specific information. In particular, we believe there should be a shift away from phenomenological models (particularly non-first-order models) in favor of models that provide a deeper understanding of the defects involved and the role played by them. Investigating and elucidating the roles and predominance of defect clustering and localized transitions in high-sensitivity TL/OSL materials may also play a key role towards a more guided "defect engineering" of new material.

Our intent has been to support a more efficient and systematic development of new TL/OSL materials, potentially offering properties currently not available in existing ones. Some of these properties may not only satisfy the needs identified in this article, but perhaps open the possibility of new, not-yet-envisioned applications of TL/OSL materials.

Declaration of competing interest

The authors declare that they have no known competing financial interests or personal relationships that could have appeared to influence the work reported in this paper.

Data availability

No data was used for the research described in the article.

Acknowledgements

The authors also would like to thank Leonardo França and Luiz Jacobsohn for comments on the manuscript.

References

Ahmed, M.F., Eller, S., Schnell, E., Ahmad, S., Akselrod, M.S., Yukihara, E.G., 2014. Development of a 2D dosimetry system based on the optically stimulated luminescence of Al_2O_3. Radiat. Meas. 71, 187–192.

Ahmed, M.F., Shrestha, N., Ahmad, S., Schnell, E., Akselrod, M.S., Yukihara, E.G., 2017. Demonstration of 2D dosimetry using Al_2O_3 optically stimulated luminescence films for therapeutic megavoltage x-ray and ion beams. Radiat. Meas. 106, 315–320.

Akselrod, M.S., Kortov, V.S., Kravetsky, D.J., Gotlib, V.I., 1990. Highly sensitive thermoluminescent anion-defect α-Al_2O_3:C single crystal detectors. Radiat. Prot. Dosim. 33, 119–122.

Akselrod, M.S., Kouwenberg, J., 2018. Fluorescent nuclear track detectors - review of past, present and future of the technology. Radiat. Meas. 117, 35–51.

Akselrod, M.S., Lucas, A.C., Polf, J.C., Mckeever, S.W.S., 1998. Optically stimulated luminescence of Al_2O_3. Radiat. Meas. 29, 391–399.

Al-Senan, R.M., Hatab, M.R., 2011. Characteristics of an OSLD in the diagnostic energy range. Med. Phys. 38, 4396–4405.

Altunal, V., Guckan, V., Ozdemir, A., Ekicibil, A., Karadag, F., Yegingil, I., Zydhachevskyy, Y., Yegingil, Z., 2021. A systematic study on luminescence characterization of lanthanide-doped BeO ceramic dosimeters. J. Alloys Compd. 876.

Andreo, P., Burns, D.T., Nahum, A.E., Seuntjens, J., Attix, F.H., 2017. Fundamentals of Ionizing Radiation Dosimetry. Wiley.

Antonov-Romanovskii, V.V., Keirum-Markus, I.F., Poroshina, M.S., Trapeznikova, Z.A., 1955. IR Stimulable Phosphors. Conference of the Academy of Sciences of the USSR on the Peaceful Uses of Atomic Energy, Moscow, pp. 239–250.

Armstrong, P., Mah, M., Ross, H., Talghader, J., 2018. Individual microparticle measurements for increased resolution of thermoluminescent temperature sensing. IEEE Sensor. J. 18, 4422–4428.

Attix, F.H., 2004. Introduction to Radiological Physics and Radiation Dosimetry. Wiley-VCH, Weinheim.

Awata, S., Tanaka, T., Fukuda, Y., 1999. Thermoluminescence and thermally stimulated exoelectron emission from CaF_2/CaO dual phases doped with lanthanide oxides for UV-ray irradiation. Phys. Status Solidi A 174, 541–549.

Bandyopadhyay, P.K., Russell, G.W., Chakrabarti, K., 1999. Optically stimulated luminescence in KCl:Cu x-irradiated at room temperature. Radiat. Meas. 30, 51–57.

Barve, R.A., Patil, R.R., Moharil, S.V., Gaikwad, N.P., Bhatt, B.C., Pradeep, R., Mishra, D. R., Kulkarni, M.S., 2015. Na_2SiF_6:Cu,P: a new OSL phosphor for the radiation dosimetric applications. Radiat. Prot. Dosim. 163, 439–445.

Bastani, S., Oliveira, L.C., Yukihara, E.G., 2019. Development and characterization of lanthanide-doped $CaSO_4$ for temperature sensing applications. Opt. Mater. 92, 273–283.

Berger, T., Hajek, M., Schoner, W., Fugger, M., Vana, N., Akatov, Y., Shurshakov, V., Arkhangelsky, V., Kartashov, D., 2002. Application of the high-temperature ratio method for evaluation of the depth distribution of dose equivalent in a water-filled phantom on board Space Station Mir. Radiat. Prot. Dosim. 100, 503–506.

Bhatt, B.C., Kulkarni, M.S., 2014. Thermoluminescent phosphors for radiation dosimetry. In: Virk, H.S. (Ed.), Luminescence Related Phenomena and Their Applications, pp. 179–227.

Bilski, P., Budzanowski, M., Olko, P., Mandowska, E., 2004. LiF:Mg,Ti (MTT) TL Detectors optimised for high-LET radiation dosimetry. Radiat. Meas. 38, 427–430.

Bilski, P., Cybulski, T., Puchalska, M., Ptaszkiewicz, M., 2008. Sensitivity loss and recovery for individual TL peaks in LiF:Mg,Ti and LiF:Mg,Cu,P after high-dose irradiation. Radiat. Meas. 43, 357–360.

Bilski, P., Mrozik, A., Kłosowski, M., Gieszczyk, W., Zorenko, Y., Kamada, K., Yoshikawa, A., Sidletskiy, O., 2021. New efficient OSL detectors based on the crystals of Ce^{3+} doped $Gd_3Al_{5-x}Ga_xO_{12}$ mixed garnet. Mater. Sci. Eng., B 273, 115448.

Bilski, P., Olko, P., Budzanowski, M., Ochab, E., Waligórski, M.P.R., 1999. Optimisation of LiF:Mg,Ti detectors for dosimetry in proton radiotherapy. Radiat. Prot. Dosim. 85, 367–371.

Blasse, G., Grabmaier, B.C., 1994. Luminescent Materials. Springer, Heidelberg.

Bos, A.J.J., 2001a. High sensitivity thermoluminescence dosimetry. Nucl. Instrum. Methods Phys. Res. B 184, 3–28.

Bos, A.J.J., 2001b. On the energy conversion in thermoluminescence dosimetry materials. Radiat. Meas. 33, 737–744.

Bøtter-Jensen, L., McKeever, S.W.S., Wintle, A.G., 2003. Optically Stimulated Luminescence Dosimetry. Elsevier, Amsterdam.

Brant, A.T., Buchanan, D.A., McClory, J.W., Dowben, P.A., Adamiv, V.T., Burak, Y.V., Halliburton, L.E., 2013. EPR identification of defects responsible for thermoluminescence in Cu-doped lithium tetraborate ($Li_2B_4O_7$) crystals. J. Lumin. 139, 125–131.

Brant, A.T., Kananan, B.E., Murari, M.K., McClory, J.W., Petrosky, J.C., Adamiv, V.T., Burak, Y.V., Dowben, P.A., Halliburton, L.E., 2011. Electron and hole traps in Ag-doped lithium tetraborate ($Li_2B_4O_7$) crystals. J. Appl. Phys. 110.

Buchanan, D.A., Holston, M.S., Brant, A.T., McClory, J.W., Adamiv, V.T., Burak, Y.V., Halliburton, L.E., 2014. Electron paramagnetic resonance and thermoluminescence study of Ag^{2+} ions in $Li_2B_4O_7$ crystals. J. Phys. Chem. Solid. 75, 1347–1353.

Bulur, E., Göksu, H.Y., 1998. OSL from BeO ceramics: new observations from an old material. Radiat. Meas. 29, 639–650.

Bulur, E., Yeltik, A., 2010. Optically stimulated luminescence from BeO ceramics: an LM-OSL study. Radiat. Meas. 45, 29–34.

Cernea, M., Secu, M., Secu, C.E., Baibarac, M., Vasile, B.S., 2011. Structural and thermoluminescence properties of undoped and Fe-doped-TiO_2 nanopowders processed by sol–gel method. J. Nanoparticle Res. 13, 77–85.

Chen, R., McKeever, S.W.S., 1994. Characterization of nonlinearities in the dose dependence of thermoluminescence. Radiat. Meas. 23, 667–673.

Chen, R., McKeever, S.W.S., 1997. Theory of Thermoluminescence and Related Phenomena. World Scientific Publishing Co., Singapore.

Chen, R., Pagonis, V., 2011. Thermally and Optically Stimulated Luminescence: A Simulation Approach. John Wiley & Sons Ltd., Chichester, West Sussex, UK.

Chernov, V., Salas-Castillo, P., Diaz-Torres, L.A., Zuniga-Rivera, N.J., Ruiz-Torres, R., Melendrez, R., Barboza-Flores, M., 2019. Thermoluminescence and infrared stimulated luminescence in long persistent monoclinic $SrAl_2O_4$:Eu^{2+},Dy^{3+} and $SrAl_2O_4$:Eu^{2+},Nd^{3+} phosphors. Opt. Mater. 92, 46–52.

Christensen, J.B., Togno, M., Bossin, L., Pakari, O.V., Safai, S., Yukihara, E.G., 2022. Improved simultaneous LET and dose measurements in proton beams of clinical relevancy using Al_2O_3:C OSL detectors. Sci. Rep. 12, 8262.

Christensen, J.B., Togno, M., Nesteruk, K., Psoroulas, S., Meer, D., Weber, D., Lomax, T., Yukihara, E.G., Safai, S., 2021. Al_2O_3:C optically stimulated luminescence dosimeters (OSLDs) for ultra-high dose rate proton dosimetry. Phys. Med. Biol. 66, 085003.

Chumak, V., Morgun, A., Zhydachevskii, Y., Ubizskii, S., Voloskiy, V., Bakhanova, O., 2017. Passive system characterizing the spectral composition of high dose rate workplace fields: potential application of high Z OSL phosphors. Radiat. Meas. 106, 638–643.

Coeck, M., Vanhavere, F., Khaidukov, N., 2002. Thermoluminescent characteristics of $LiKYF_5$:Pr^{3+} and KYF_4:Tm^{3+} crystals for applications in neutron and gamma dosimetry. Radiat. Prot. Dosim. 100, 221–224.

Coleman, A.C., Yukihara, E.G., 2018. On the validity and accuracy of the initial rise method investigated using realistically simulated thermoluminescence curves. Radiat. Meas. 117, 70–79.

Currie, L.A., 1968. Limits for qualitative detection and quantitative determination - application to radiochemistry. Anal. Chem. 40, 586–593.

Daniels, F., Boyd, C.A., Saunders, D.F., 1953. Thermoluminescence as a research tool. Science 117, 343–349.

Danilkin, M., Kerikmäe, M., Kirillov, A., Lust, A., Ratas, A., Paama, L., Seeman, V., 2006. Thermoluminescent dosimeter $Li_2B_4O_7$:Mn,Si – a false-dose problem. Proc. Est. Acad. Sci., Chem. 55, 123–131.

Dhabekar, B., Rawat, N.S., Gaikwad, N., Kadam, S., Koul, D.K., 2017. Dosimetric characterization of highly sensitive OSL phosphor: $LiCaAlF_6$:Eu. Y. Radiat. Meas. 107, 7–13.

Dhadade, I.H., Moharil, S.V., Dhoble, S.J., Rahangdale, S.R., 2016. Combustion synthesis and thermoluminescence in $YAlO_3$:Dy^{3+}. AIP Conf. Proc. 1728, 020174.

Dobrowolska, A., Bos, A.J.J., Dorenbos, P., 2014. Electron tunnelling phenomena in YPO_4:Ce, Ln (Ln = Er, Ho, Nd, Dy). J. Phys. D: Appl. Phys. 47.

Dorenbos, P., 2000a. 5d-level energies of Ce^{3+} and the crystalline environment. I. Fluoride compounds. Phys. Rev. B 62, 15640–15649.

Dorenbos, P., 2000b. The 5d level position of the trivalent lanthanides in inorganic compounds. J. Lumin. 91, 155–176.

Dorenbos, P., 2003. f -> d transition energies of divalent lanthanides in inorganic compounds. J. Phys. Condens. Matter 15, 575–594.

Dorenbos, P., 2019. The nephelauxetic effect on the electron binding energy in the $4f^q$ ground state of lanthanides in compounds. J. Lumin. 214, 116536.

Dorenbos, P., 2020. [INVITED] Improved parameters for the lanthanide $4f^q$ and $4f^{q-1}5d$ curves in HRBE and VRBE schemes that takes the nephelauxetic effect into account. J. Lumin. 222, 117164.

Dorenbos, P., Bos, A.J.J., 2008. Lanthanide level location and related thermoluminescence phenomena. Radiat. Meas. 43, 139–145.

Dotzler, C., Williams, G.V.M., Rieser, U., Robinson, J., 2009. Photoluminescence, optically stimulated luminescence, and thermoluminescence study of $RbMgF_3$:Eu^{2+}. J. Appl. Phys. 105.

Doull, B.A., Oliveira, L.C., Wang, D.Y., Milliken, E.D., Yukihara, E.G., 2014. Thermoluminescent properties of lithium borate, magnesium borate and calcium sulfate developed for temperature sensing. J. Lumin. 146, 408–417.

Doull, B.A., Oliveira, L.C., Yukihara, E.G., 2013. Effect of annealing and fuel type on the thermoluminescent properties of $Li_2B_4O_7$ synthesized by solution combustion synthesis. Radiat. Meas. 56, 167–170.

Fasoli, M., Vedda, A., Nikl, M., Jiang, C., Uberuaga, B.P., Andersson, D.A., McClellan, K. J., Stanek, C.R., 2011. Band-gap engineering for removing shallow traps in rare-earth $Lu_3Al_5O_{12}$ garnet scintillators using Ga^{3+} doping. Phys. Rev. B 84.

Flint, D.B., Granville, D.A., Sahoo, N., McEwen, M., Sawakuchi, G.O., 2016. Ionization density dependence of the curve shape and ratio of blue to UV emissions of Al_2O_3:C optically stimulated luminescence detectors exposed to 6-MV photon and therapeutic proton beams. Radiat. Meas. 89, 35–43.

Gaikwad, S., More, Y., Patil, R.R., Kulkarni, M.S., Bhatt, B.C., Moharil, S.V., 2016a. Optically stimulated luminescence in doped $K_3Na(SO_4)_2$ phosphors. Radiat. Meas. 93, 20–27.

Gaikwad, S.U., Patil, R.R., Kulkarni, M.S., Bhatt, B., Moharil, S.V., 2016b. Optically stimulated luminescence in doped NaF. Appl. Radiat. Isot. 111, 75–79.

Gaikwadl, S.U., Patil, R.R., Kulkarni, M.S., Bhatt, B., Moharil, S.V., 2016. Optically stimulated luminescence in doped NaCl. In: Shekhawat, M.S., Bhardwaj, S., Suthar, B. (Eds.), International Conference on Condensed Matter and Applied Physics.

Gobrecht, H., Hofmann, D., 1966. Spectroscopy of traps by fractional glow technique. J. Phys. Chem. Solid. 27, 509–522.

Guckan, V., Altunal, V., Ozdemir, A., Tsiumra, V., Zhydachevskyy, Y., Yegingil, Z., 2020. Calcination effects on europium doped zinc oxide as a luminescent material synthesized via sol-gel and precipitation methods. J. Alloys Compd. 823, 153878.

Guidelli, E.J., Baffa, O., Clarke, D.R., 2015. Enhanced UV emission from silver/ZnO and gold/ZnO core-shell nanoparticles: photoluminescence, radioluminescence, and optically stimulated luminescence. Sci. Rep. 5, 14004.

Guimarães, C.C., Okuno, E., 2003. Blind performance testing of personal and environmental dosimeters based on TLD-100 and natural CaF_2:NaCl. Radiat. Meas. 37, 127–132.

Gustafson, T.D., Milliken, E.D., Jacobsohn, L.G., Yukihara, E.G., 2019. Progress and challenges towards the development of a new optically stimulated luminescence (OSL) material based on MgB_4O_7:Ce,Li. J. Lumin. 212, 242–249.

Hajek, M., Berger, T., Bergmann, R., Vana, N., Uchihori, Y., Yasuda, N., Kitamura, H., 2008. LET dependence of thermoluminescent efficiency and peak height ratio of CaF2 : Tm. Radiat. Meas. 43, 1135–1139.

Hatwar, L.R., Wankhede, S.P., Moharil, S.V., Muthal, P.L., Dhopte, S.M., 2014. Luminescence in $Li_2BaP_2O_7$. Luminescence 30, 714–718.

Hazelton, J.R., Yukihara, E.G., Jacobsohn, L.G., Blair, M.W., Muenchausen, R.E., 2010. Feasibility of using oxyorthosilicates as optically stimulated luminescence detectors. Radiat. Meas. 45, 681–683.

Hemam, R., Singh, L.R., Singh, S.D., Sharan, R.N., 2018. Preparation of CaB_4O_7 nanoparticles doped with different concentrations of Tb^{3+}: photoluminescence and thermoluminescence/optically stimulated luminescence study. J. Lumin. 197, 399–405.

Henderson, B., Imbusch, G.F., 1989. Optical Spectroscopy of Inorganic Solids. Claredon Press, Oxford.

Holston, M.S., Ferguson, I.P., Giles, N.C., McClory, J.W., Halliburton, L.E., 2015a. Identification of defects responsible for optically stimulated luminescence (OSL) from copper-diffused $LiAlO_2$ crystals. J. Lumin. 164, 105–111.

Holston, M.S., McClory, J.W., Giles, N.C., Halliburton, L.E., 2015b. Radiation-induced defects in $LiAlO_2$ crystals: holes trapped by lithium vacancies and their role in thermoluminescence. J. Lumin. 160, 43–49.

Horowitz, Y., Oster, L., Eliyahu, I., 2018. Review of dose-rate effects in the thermoluminescence of LiF:Mg,Ti (Harshaw). Radiat. Prot. Dosim. 179, 184–188.

Horowitz, Y.S., 1981. The theoretical and microdosimetric basis of thermoluminescence and applications to dosimetry. Phys. Med. Biol. 26, 765–824.

Horowitz, Y.S., Moscovitch, M., 2013. Highlights and pitfalls of 20 years of application of computerised glow curve analysis to thermoluminescence research and dosimetry. Radiat. Prot. Dosim. 153, 1–22.

Horowitz, Y.S., Oster, L., Eliyahu, I., 2019. The saga of the thermoluminescence (TL) mechanisms and dosimetric characteristics of LiF:Mg,Ti (TLD-100). J. Lumin. 214.

Horowitz, Y.S., Yossian, D., 1995. Computerised glow curve deconvolution: application to thermoluminescence dosimetry. Radiat. Prot. Dosim. 60, 1-114.

IAEA, 2000. IAEA TRS-398: Absorbed Dose Determination in External Beam Radiotherapy: an International Code of Practice for Dosimetry Based on Standards of Absorbed Dose to Water. International Atomic Energy Agency, Vienna.

ICRP, 2013. ICRP publication 123: assessment of radiation exposure of astronauts in space. Ann. ICRP 42.

ICRU, 1993. ICRU Report 51: Quantities and Units in Radiation Protection Dosimetry. International Comission on Radiation Units and Measurements, Bethesda, MD.

ICRU, 2001. ICRU Report 66: determination of operational dose equivalent quantities for neutrons. J. ICRU 1, 1–93.

IEC, 2020. IEC 62387:2020-01: Radiation Protection Instrumentation – Dosimetry Systems with Integrating Passive Detectors for Individual, Workplace and Environmental Monitoring of Photon and Beta Radiation. International Electrotechnical Commission, Geneva.

ISO/ASTM, 2013a. ISO/ASTM 51261:2013: Practice for Calibration of Routine Dosimetry Systems for Radiation Processing. International Organization for Standardization/ASTM International.

ISO/ASTM, 2013b. ISO/ASTM 51956: Practice for Use of a Thermoluminescence-Dosimetry System (TLD System) for Radiation Processing. International Organization for Standardization/ASTM International.

Jacobsohn, L.G., Blair, M.W., Tornga, S.C., Brown, L.O., Bennett, B.L., Muenchausen, R. E., 2008. Y_2O_3:Bi nanophosphor: solution combustion synthesis, structure, and luminescence. J. Appl. Phys. 104, 124303.

Jaffray, D., Carlone, M., Menard, C., Breen, S., 2010. Image-guided Radiation Therapy: Emergence of MR-Guided Radiation Treatment (MRgRT) Systems, Medical Imaging 2010: Physics of Medical Imaging. International Society for Optics and Photonics, 762202.

Jain, M., Ankjærgaard, C., 2011. Towards a non-fading signal in feldspar: Insight into charge transport and tunnelling from time-resolved optically stimulated luminescence. Radiat. Meas. 46, 292–309.

Jain, M., Sohbati, R., Guralnik, B., Murray, A.S., Kook, M., Lapp, T., Prasad, A.K., Thomsen, K.J., Buylaert, J.P., 2015. Kinetics of infrared stimulated luminescence from feldspars. Radiat. Meas. 81, 242–250.

Jensen, M.L., Nyemann, J.S., Muren, L.P., Julsgaard, B., Balling, P., Turtos, R.M., 2022. Optically stimulated luminescence in state-of-the-art LYSO:Ce scintillators enables high spatial resolution 3D dose imaging. Sci. Rep. 12, 8301.

Joos, J.J., Korthout, K., Amidani, L., Glatzel, P., Poelman, D., Smet, P.F., 2020. Identification of Dy^{3+}/Dy^{2+} as electron trap in persistent phosphors. Phys. Rev. Lett. 125, 033001.

Kalef-Ezra, J., Horowitz, Y.S., 1982. Heavy charged particle thermoluminescence dosimetry: track structure theory and experiments. Int. J. Appl. Radiat. Isot. 33, 1085–1100.

Kananen, B.E., Maniego, E.S., Golden, E.M., Giles, N.C., McClory, J.W., Adamiv, V.T., Burak, Y.V., Halliburton, L.E., 2016. Optically stimulated luminescence (OSL) from Ag-doped $Li_2B_4O_7$ crystals. J. Lumin. 177, 190–196.

Kananen, B.E., McClory, J.W., Giles, N.C., Halliburton, L.E., 2018. Copper-doped lithium triborate (LiB_3O_5) crystals: a photoluminescence, thermoluminescence, and electron paramagnetic resonance study. J. Lumin. 194, 700–705.

Karsch, L., Beyureuther, E., Burris-Mog, T., Kraft, S., Richter, C., Zeil, K., 2012. Dose rate dependence for different dosimeters and detectors: TLD, OSL, EBT films, and diamond detectors. Med. Phys. 5, 2447–2455.

Katayama, Y., Hashimoto, A., Xu, J., Ueda, J., Tanabe, S., 2017. Thermoluminescence investigation on $Y_3Al_{5-x}Ga_xO_{12}$: Ce^{3+}-Bi^{3+} green persistent phosphors. J. Lumin. 183, 355–359.

Kim, H., Yu, H., Discher, M., Kim, M.C., Choi, Y., Lee, H., Lee, J.T., Lee, H., Kim, Y.S., Kim, H.S., Lee, J., 2022. A small-scale realistic inter-laboratory accident dosimetry comparison using the TL/OSL from mobile phone components. Radiat. Meas. 150.

Kitagawa, Y., Yukihara, E.G., Tanabe, S., 2021. Development of Ce^{3+} and Li^+ co-doped magnesium borate glass ceramics for optically stimulated luminescence dosimetry. J. Lumin. 232, 117847.

Kitis, G., Gomes-Ros, J.M., Tuyn, J.W.N., 1998. Thermoluminescence glow-curve deconvolution functions for first, second and general order kinetics. J. Phys. D Appl. Phys. 31, 2636–2641.

Knoll, G.F., 2000. Radiation Detection and Measurements. John Wiley & Sons, Inc.

Kortov, V.S., 2010. Nanophosphors and outlooks for their use in ionizing radiation detection. Radiat. Meas. 45, 512–515.

Kry, S.F., Alvarez, P., Cygler, J.E., DeWerd, L.A., Howell, R.M., Meeks, S., O'Daniel, J., Reft, C., Sawakuchi, G., Yukihara, E.G., Mihailidis, D., 2020. AAPM TG 191 clinical use of luminescent dosimeters: TLDs and OSLDs. Med. Phys. 47, e19–e51.

Kui, H.W., Lo, D., Tsang, Y.C., Khaidukov, N.M., Makhov, V.N., 2006. Thermoluminescence properties of double potassium yttrium fluorides singly doped with Ce^{3+}, Tb^{3+}, Dy^{3+} and Tm^{3+} in response to alpha and beta irradiation. J. Lumin. 117, 29–38.

Kumar, P., Bahl, S., Sahare, P.D., Kumar, S., Singh, M., 2015. Optically stimulated luminescence (OSL) response of Al_2O_3:C, BaFCl:Eu and $K_2Ca_2(SO_4)_3$:Eu phosphors. Radiat. Prot. Dosim. 167, 453–460.

Lastusaari, M., Bos, A.J.J., Dorenbos, P., Laamanen, T., Malkamäki, M., Rodrigues, L.C. V., Hölsä, J., 2015. Wavelength-sensitive energy storage in $Sr_3MgSi_2O_8$:Eu^{2+},Dy^{3+}. J. Therm. Anal. Calorim. 121, 29–35.

Le Masson, N.J.M., Bos, A.J.J., Van Eijk, C.W.E., 2001. Optically stimulated luminescence in hydrated magnesium sulfates. Radiat. Meas. 33, 693–697.

Le Masson, N.J.M., Bos, A.J.J., Van Eijk, C.W.E., Furetta, C., Chaminade, J.P., 2002. Optically and thermally stimulated luminescence of $KMgF_3$:Ce^{3+} and $NaMgF_3$:Ce^{3+}. Radiat. Prot. Dosim. 100, 229–234.

Le Masson, N.J.M., Czapla, Z., Bos, A.J.J., Brouwer, J.C., van Eijk, C.W.E., 2004. Luminescence and OSL study of the inorganic compounds Tl^+-doped $(NH_4)_2BeF_4$ and $(NH_4)_2SiF_6$. Radiat. Meas. 38, 549–552.

Leblans, P., Vandenbroucke, D., Willems, P., 2011. Storage phosphors for medical imaging. Materials 4, 1034–1086.

Lee, J.I., Pradhan, A.S., Kim, J.L., Kim, B.H., Yim, K.S., 2008. Response of (LiF)-Li-6:Mg, Cu,Si and (LiF)-Li-7:Mg,Cu,Si TLD pairs to the neutrons and photon mixtures. J. Nucl. Sci. Technol. 233–236.

Lee, J.I., Yang, J.S., Kim, J.L., Pradhan, A.S., Lee, J.D., Chung, K.S., Choe, H.S., 2006. Dosimetric characteristics of LiF:Mg,Cu,Si thermoluminescent materials. Appl. Phys. Lett. 89.

Li, H.H., Driewer, J.P., Han, Z., Low, D.A., Yang, D., Xiao, Z., 2014. Two-dimensional high spatial-resolution dosimeter using europium doped potassium chloride: a feasibility study. Phys. Med. Biol. 59, 1899–1909.

Liu, Y., Chen, Z., Fan, Y., Ba, W., Lu, W., Guo, Q., Pan, S., Chang, A., Tang, X., 2008a. Design of a novel optically stimulated luminescent dosimeter using alkaline earth sulfides doped with SrS:Eu,Sm materials. Prog. Nat. Sci. 18, 1203–1207.

Liu, Y.P., Chen, Z.Y., Ba, W.Z., Fan, Y.W., Guo, Q., Yu, X.F., Chang, A.M., Lu, W., Du, Y. Z., 2008b. Optically stimulated luminescence dosimeter based on CaS:Eu,Sm. Nucl. Sci. Tech. 19, 113–116.

Luchechko, A., Zhydachevskyy, Y., Maraba, D., Bulur, E., Ubizskii, S., Kravets, O., 2018. TL and OSL properties of Mn^{2+}-doped $MgGa_2O_4$ phosphor. Opt. Mater. 78, 502–507.

Luo, H.D., Bos, A.J.J., Dorenbos, P., 2016. Controlled electron-hole trapping and detrapping process in GdAlO3 by valence band engineering. J. Phys. Chem. C 120, 5916–5925.

Luo, L.Z., 2008. Extensive fade study of Harshaw LiF TLD materials. Radiat. Meas. 43, 365–370.

Luo, Z.L., Geng, B., Bao, J., Gao, C., 2005. Parallel solution combustion synthesis for combinatorial materials studies. J. Comb. Chem. 7, 942–946.

Manimozhi, P.K., Muralidharan, G., Selvasekarapandian, S., Malathi, J., 2007. Thermoluminescence and other optical studies on RbBr:Tb^{3+} crystals. Phys. Status Solidi B 244, 726–734.

Marcazzo, J., Cruz-Zaragoza, E., Quang, V.X., Khaidukov, N.M., Santiago, M., 2011. OSL, RL and TL characterization of rare-earth ion doped K_2YF_5: application in dosimetry. J. Lumin. 131, 2711–2715.

Markey, B.G., Colyott, L.E., McKeever, S.W.S., 1995. Time-resolved optically stimulated luminescence from a-Al_2O_3:C. Radiat. Meas. 24, 457–463.

Martini, M., Fasoli, M., 2019. Luminescence and defects in quartz. In: Chen, R., Pagonis, V. (Eds.), Advances in Physics and Applications of Optically and Thermally Stimulated Luminescence. World Scientific, Singapore.

Matsuzawa, T., Aoki, Y., Takeuchi, N., Murayama, Y., 1996. New long phosphorescent phosphor with high brightness, $SrAl_2O_4$:Eu^{2+},Dy^{3+}. J. Electrochem. Soc. 143, 2670–2673.

McKeever, S.W.S., 1985. Thermoluminescence of Solids. Cambridge University Press, Cambridge.

McKeever, S.W.S., 2022. A Course in Luminescence Measurements and Analyses for Radiation Dosimetry. Wiley.

McKeever, S.W.S., Chen, C.Y., Halliburton, L.E., 1985. Point-defects and the predose effect in natural quartz. Nucl. Tracks Radiat. Meas. 10, 489–495.

McKeever, S.W.S., Jassemnejad, B., Landreth, J.F., Brown, M.D., 1986. Manganese absorption in CaF_2:Mn; I. J. Appl. Phys. 60, 1124–1130.

McKeever, S.W.S., Moscovitch, M., Townsend, P.D., 1995. Thermoluminescence Dosimetry Materials: Properties and Uses. Nuclear Technology Publishing, Ashford.

Medlin, W.L., 1961. Thermoluminescence in anhydrite. J. Phys. Chem. Solid. 18, 238–252.

Menon, S., Dhabekar, B., Alagu Raja, E., More, S.P., Gundu Rao, T.K., Kher, R.K., 2008. TSL, OSL and ESR studies in $ZnAl_2O_4$:Tb phosphor. J. Lumin. 128, 1673–1678.

Merz, J.L., Pershan, P.S., 1967a. Charge conversion of irradiated rare-earth ions in CaF_2. II. Thermoluminescent spectra. Phys. Rev. 162, 235–247.

Merz, J.L., Pershan, P.S., 1967b. Charge conversion of irradiated rare-earth ions in calcium fluoride. I. Phys. Rev. 162, 217–235.

Milliken, E.D., Oliveira, L.C., Denis, G., Yukihara, E.G., 2012. Testing a model-guided approach to the development of new thermoluminescent materials using YAG:Ln produced by solution combustion synthesis. J. Lumin. 132, 2495–2504.

Missous, O., Loup, F., Prevost, H., Fesquet, J., Gasiot, J., 1992. Effect of dopant concentration on optically stimulated luminescence properties of MgS. J. Alloys Compd. 180, 209–213.

Mittani, J.C., Prokić, M., Yukihara, E.G., 2008. Optically stimulated luminescence and thermoluminescence of terbium-activated silicates and aluminates. Radiat. Meas. 43, 323–326.

Mittani, J.C.R., da Silva, A.A.R., Vanhavere, F., Akselrod, M.S., Yukihara, E.G., 2007. Investigation of neutron converters for production of optically stimulated luminescence (OSL) neutron dosimeters using Al_2O_3:C. Nucl. Instrum. Methods Phys. Res. B 260, 663–671.

Moscovitch, M., 1999. Personnel dosimetry using LiF:Mg,Cu,P. Radiat. Prot. Dosim. 85, 49–56.

Moscovitch, M., Tawil, R.A., Svinkin, M., 1993. Light induced fading in α-Al_2O_3:C. Radiat. Prot. Dosim. 47, 251–253.

Muñoz, I.D., Avila, O., Gamboa-deBuen, I., Brandan, M.E., 2015. Evolution of the CaF_2: Tm (TLD-300) glow curve as an indicator of beam quality for low-energy photon beams. Phys. Med. Biol. 60, 2135–2144.

Nakajima, T., Murayama, Y., Matsuzawa, T., Koyano, A., 1978. Development of a new highly sensitive LiF thermoluminescence dosimeter and its applications. Nucl. Instrum. Methods 157, 155–162.

Nakauchi, D., Okada, G., Yanagida, T., 2016. Scintillation, OSL and TSL properties of yttria stabilized zirconia crystal. J. Lumin. 172, 61–64.

Nambi, K.S.V., Bapat, V.N., Ganguly, A.K., 1974. Thermoluminescence of $CaSO_4$ doped with rare earths. J. Phys. C Solid State Phys. 7, 4403–4415.

Nanto, H., 2018. Photostimulable storage phosphor materials and their application to radiation monitoring. Sensor. Mater. 30, 327–337.

Noll, M., Vana, N., Schöner, W., Fugger, M., Brandl, H., 1996. Dose measurements in mixed (n,gamma) radiation fields in aircraft with TLDs under consideration of the high temperature ratio. Radiat. Prot. Dosim. 66, 119–124.

Nunes, M.C.S., Lima, L.S., Yoshimura, E.M., França, L.V.S., Baffa, O., Jacobsohn, L.G., Malthez, A.L.M.C., Kunzel, R., Trindade, N.M., 2020. Characterization of the optically stimulated luminescence (OSL) response of beta-irradiated alexandrite-polymer composites. J. Lumin. 226, 117479.

Nyemann, J.S., Turtos, R.M., Julsgaard, B., Muren, L.P., Balling, P., 2020. Optical characterization of LiF:Mg,Cu,P - towards 3D optically stimulated luminescence dosimetry. Radiat. Meas. 138, 106390.

Okada, G., Kasap, S., Yanagida, T., 2016. Optically- and thermally-stimulated luminescences of Ce-doped SiO_2 glasses prepared by spark plasma sintering. Opt. Mater. 61, 15–20.

Oliveira, L.C., Baffa, O., 2017. A new luminescent material based on CaB_6O_{10}:Pb to detect radiation. J. Lumin. 181, 171–178.

Oliveira, L.C., Yukihara, E.G., Baffa, O., 2019. Lanthanide-doped MgO: a case study on how to design new phosphors for dosimetry with tailored luminescence properties. J. Lumin. 209, 21–30.

Olko, P., 2002. Microdosimetric Modelling of Physical and Biological Detectors. The Henryk Niewodniczański Institute of Nuclear Physics, Kraków.

Olko, P., Bilski, P., 2020. Microdosimetric understanding of dose response and relative efficiency of thermoluminescence detectors. Radiat. Prot. Dosim. 192, 165–177.

Opanowicz, A., 1989. On the kinetics order of thermoluminescence in insulating crystals. Phys. Status Solidi A 116, 343–348.

Orante-Barrón, V.R., Cruz-Vázquez, C., Bernal, R., Denis, G., Yukihara, E.G., 2010. Thermoluminescence properties of novel La_2O_3 phosphor obtained by solution combustion synthesis. MRS Proceedings 1278, S08–S74.

Orante-Barrón, V.R., Oliveira, L.C., Kelly, J.B., Milliken, E.D., Denis, G., Jacobsohn, L.G., Puckette, J., Yukihara, E.G., 2011. Luminescence properties of MgO produced by Solution Combustion Synthesis and doped with lanthanides and Li. J. Lumin. 131, 1058–1065.

Ozdemir, A., Altun, V., Guckan, V., Can, N., Kurt, K., Yegingil, I., Yegingil, Z., 2018. Characterization and some fundamental features of Optically Stimulated Luminescence measurements of silver activated lithium tetraborate. J. Lumin. 202, 136–146.

Pagonis, V., Kitis, G., 2012. Prevalence of first-order kinetics in thermoluminescence materials: an explanation based on multiple competition processes. Phys. Status Solidi B 249, 1590–1601.

Palan, C.B., Bajaj, N.S., Omanwar, S.K., 2016a. Luminescence properties of Eu^{2+} doped SrB_4O_7 phosphor for radiation dosimetry. Mater. Res. Bull. 76, 216–221.

Palan, C.B., Bajaj, N.S., Omanwar, S.K., 2016b. Luminescence properties of terbium-doped Li_3PO_4 phosphor for radiation dosimetry. Bull. Mater. Sci. 39, 1619–1623.

Palan, C.B., Bajaj, N.S., Omanwar, S.K., 2016c. Synthesis and luminescence properties of $KSrPO_4:Eu^{2+}$ phosphor for radiation dosimetry. In: Shekhawat, M.S., Bhardwaj, S., Suthar, B. (Eds.), International Conference on Condensed Matter and Applied Physics.

Palan, C.B., Bajaj, N.S., Soni, A., Omanwar, S.K., 2016d. A novel $KMgPO_4:Tb^{3+}$ (KMPT) phosphor for radiation dosimetry. J. Lumin. 176, 106–111.

Palan, C.B., Koparkar, K.A., Bajaj, N.S., Omanwar, S.K., 2016e. Synthesis and TL/OSL properties of $CaSiO_3$:Ce biomaterial. Mater. Lett. 175, 288–290.

Palan, C.B., Koparkar, K.A., Bajaj, N.S., Soni, A., Omanwar, S.K., 2016f. A novel high sensitivity $KCaPO_4:Ce^{3+}$ phosphor for radiation dosimetry. Res. Chem. Intermed. 42, 7637–7649.

Palan, C.B., Koparkar, K.A., Bajaj, N.S., Soni, A., Omanwar, S.K., 2016g. Synthesis and TL/OSL properties of a novel high-sensitive blue-emitting $LiSrPO_4:Eu^{2+}$ phosphor for radiation dosimetry. Appl. Phys. A 122.

Pan, L., Sholom, S., McKeever, S.W.S., Jacobsohn, L.G., 2021. Magnesium aluminate spinel for optically stimulated luminescence dosimetry. J. Alloys Compd. 880, 160503.

Patle, A., Patil, R.R., Kulkarni, M.S., Bhatt, B.C., Moharil, S.V., 2015a. Development of europium doped $BaSO_4$ TL OSL dual phosphor for radiation dosimetry applications. In: Sinha, M.M., Verma, S.S. (Eds.), Advanced Materials and Radiation Physics.

Patle, A., Patil, R.R., Kulkarni, M.S., Bhatt, B.C., Moharil, S.V., 2015b. Highly sensitive Europium doped $SrSO_4$ OSL nanophosphor for radiation dosimetry applications. Opt. Mater. 48, 185–189.

Pedroza-Montero, M., Castañeda, B., Meléndrez, R., Piters, T.M., Barboza-Flores, M., 2000. Thermoluminescence, optically stimulated luminescence and defect creation in europium doped KCl and KBr crystals. Phys. Status Solidi B 220, 671–676.

Pradhan, A.S., Lee, J.I., Kim, J.L., 2008. Recent developments of optically stimulated luminescence materials and techniques for radiation dosimetry and clinical applications. J. Med. Phys. 33, 85–99.

Ptaszkiewicz, M., 2007. Long-term fading of LiF:Mg,Cu,P and LiF:Mg,Ti thermoluminescence detectors with standard and modified activator composition. Radiat. Meas. 42, 605–608.

Quilty, J.W., Edgar, A., Schierning, G., 2008. Photostimulated luminescence and thermoluminescence in europium-doped barium magnesium fluoride. Curr. Appl. Phys. 8, 420–424.

Rivera, T., Furetta, C., Azorin, J., Barrera, M., Soto, A.M., 2007. Thermoluminescence (TL) of europium-doped ZrO_2 obtained by sol-gel method. Radiat. Eff. Defects Solids 162, 379–383.

Sądel, M., Bilski, P., Kłosowski, M., Sankowska, M., 2020a. A new approach to the 2D radiation dosimetry based on optically stimulated luminescence of LiF:Mg,Cu,P. P. Radiat. Meas. 133, 106293.

Sądel, M., Bilski, P., Sankowska, M., Gajewski, J., Swakoń, J., Horwacik, T., Nowak, T., Kłosowski, M., 2020b. Two-dimensional radiation dosimetry based on LiMgPO4 powder embedded into silicone elastomer matrix. Radiat. Meas. 133, 106255.

Sáez-Vergara, J.C., Romero, A.M., 1996. The influence of the heating system on the hypersensitive thermoluminescent material LiF:Mg,Cu,P (GR-200). Radiat. Prot. Dosim. 66, 431–436.

Sahare, P.D., Ali, N., Rawat, N.S., Bahl, S., Kumar, P., 2016. Dosimetry characteristics of $NaLi_2PO_4:Ce^{3+}$ OSLD phosphor. J. Lumin. 174, 22–28.

Salah, N., Habib, S.S., Khan, Z.H., Djouider, F., 2011. Thermoluminescence and photoluminescence of ZrO_2 nanoparticles. Radiat. Phys. Chem. 80, 923–928.

Sanyal, S., Akselrod, M.S., 2005. Anisotropy of optical absorption and fluorescence in Al_2O_3:C,Mg crystals. J. Appl. Phys. 98, 033518.

Sardar, M., Souza, D.N., Groppo, D.P., Caldas, L.V.E., Tufail, M., 2013. Suitability of topaz glass composites as dosimeters using optically stimulated luminescence technique. IEEE Trans. Nucl. Sci. 60, 850–854.

Sas-Bieniarz, A., Marczewska, B., Kłosowski, M., Bilski, P., Gieszczyk, W., 2020. TL, OSL and RL emission spectra of RE-doped $LiMgPO_4$ crystals. J. Lumin. 218, 116839.

Sawakuchi, G.O., Sahoo, N., Gasparian, P.B.R., Rodriguez, M.G., Archambault, L., Titt, U., Yukihara, E.G., 2010. Determination of average LET of therapeutic proton beams using Al_2O_3:C optically stimulated luminescence (OSL) detectors. Phys. Med. Biol. 55, 4963–4976.

Scarboro, S.B., Cody, D., Alvarez, P., Followill, D., Court, L., Stingo, F.C., Zhang, D., McNitt-Gray, M., Kry, S.F., 2015. Characterization of the nanoDot OSLD dosimeter in CT. Med. Phys. 42, 1797–1807.

Scarboro, S.B., Cody, D., Stingo, F.C., Alvarez, P., Followill, D., Court, L., Zhang, D., McNitt-Gray, M., Kry, S.F., 2019. Calibration strategies for use of the nanoDot OSLD in CT applications. J. Appl. Clin. Med. Phys. 20, 331–339.

Schöner, W., Vana, N., Fogger, M., 1999. The LET dependence of LiF:Mg,Ti dosemeters and its implication for LET measurements in mixed radiation fields. Radiat. Prot. Dosim. 85, 263–266.

Shivaramu, N.J., Lakshminarasappa, B.N., Nagabhushana, K.R., Coetsee, E., Swart, H.C., 2018. Correlation between thermoluminescence glow curve and emission spectra of gamma ray irradiated $LaAlO_3$. AIP Conf. Proc. (1942), 050135.

Shrestha, N., vandenbroucke, D., Leblans, P., Yukihara, E.G., 2020a. Feasibility studies on the use of MgB_4O_7:Ce,Li-based films in 2D optically stimulated luminescence dosimetry. Phys. Open 5, 100037.

Shrestha, N., Yukihara, E.G., Cusumano, D., Placidi, L., 2020b. Al_2O_3:C and Al_2O_3:C,Mg optically stimulated luminescence 2D dosimetry applied to magnetic resonance guided radiotherapy. Radiat. Meas. 138, 106439.

Soares, A.F., Tatumi, S.H., Mazzo, T.M., Rocca, R.R., Courrol, L.C., 2017. Study of morphological and luminescent properties (TL and OSL) of ZnO nanocrystals synthetized by coprecipitation method. J. Lumin. 186, 135–143.

Sommer, M., Jahn, A., Henniger, J., 2011. A new personal dosimetry system for $H_p(10)$ and $H_p(0.07)$ photon dose based on OSL-dosimetry of beryllium oxide. Radiat. Meas. 46, 1818–1821.

Sorger, D., Stadtmann, H., Sprengel, W., 2020. Fading study and readout optimization for routinely use of LiF:Mg,Ti thermoluminescent detectors for personal dosimetry. Radiat. Meas. 135.

Souza, L.F., Silva, A.M.B., Antonio, P.L., Caldas, L.V.E., Souza, S.O., d'Errico, F., Souza, D.N., 2017. Dosimetric properties of MgB_4O_7:Dy,Li and MgB_4O_7:Ce,Li for optically stimulated luminescence applications. Radiat. Meas. 106, 196–199.

Spindeldreier, C.K., Schrenk, O., Ahmed, M.F., Shrestha, N., Karger, C.P., Greilich, S., Pfaffenberger, A., Yukihara, E.G., 2017. Feasibility of dosimetry with optically stimulated luminescence detectors in magnetic fields. Radiat. Meas. 106, 346–351.

Sunta, C.M., 2015. Unraveling Thermoluminescence. Springer.

Talghader, J.J., Mah, M.L., Yukihara, E.G., Coleman, A.C., 2016. Thermoluminescent microparticle thermal history sensors. Microsyst. Nanoeng. 2, 16037.

Tang, K., 2000. Thermal loss and recovery of thermoluminescence sensitivity in LiF:Mg, Cu,P. Radiat. Prot. Dosim. 90, 449–452.

Thakre, P.S., Gedam, S.C., Dhoble, S.J., 2012. Thermoluminescence properties of gamma-irradiated $KCaSO_4Cl$: X (X = Ce, Dy, Mn or Pb). J. Mater. Sci. 47, 1860–1866.

Tochilin, E., Goldstein, N., Miller, W.G., 1969. Beryllium oxide as a thermoluminescent dosimeter. Health Phys. 16, 1–7.

Townsend, P.D., Wang, Y., McKeever, S.W.S., 2021. Spectral evidence for defect clustering: relevance to radiation dosimetry materials. Radiat. Meas. 147, 106634.

Ieee Twardak, A., Bilski, P., Zorenko, Y., Gorbenko, V., Mandowska, E., Mandowski, A., 2014a. Thermoluminescence Properties of LSO:Ce and YSO:Ce Films Grown from PbO and Bi2O3 Fluxes, IEEE International Conference on Oxide Materials for Electronic Engineering - Fabrication, Properties and Applications (OMEE). Lviv Polytechn Natl Univ, Lviv, UKRAINE, pp. 259–260.

Twardak, A., Bilski, P., Zorenko, Y., Gorbenko, V., Sidletskiy, O., 2014b. OSL dosimetric properties of cerium doped lutetium orthosilicates. Radiat. Meas. 71, 139–142.

Ueda, J., Dorenbos, P., Bos, A.J.J., Kuroishi, K., Tanabe, S., 2015. Control of electron transfer between Ce^{3+} and Cr^{3+} in the $Y_3Al_{5-x}Ga_xO_{12}$ host via conduction band engineering. J. Mater. Chem. C 3, 5642–5651.

Umisedo, N.K., Okuno, E., Cancio, F., Yoshimura, E.M., Kunzel, R., 2020. Development of a mechanically resistant fluorite-based pellet to be used in personal dosimetry. Radiat. Meas. 134, 106330.

Van den Eeckhout, K., Bos, A.J.J., Poelman, D., Smet, P.F., 2013. Revealing trap depth distributions in persistent phosphors. Phys. Rev. B 87, 045126.

Vedda, A., Fasoli, M., 2018. Tunneling recombinations in scintillators, phosphors, and dosimeters. Radiat. Meas. 118, 86–97.

Vozenin, M.C., Hendry, J.H., Limoli, C.L., 2019. Biological benefits of ultra-high dose rate FLASH radiotherapy: sleeping beauty awoken. Clin. Oncol. 31, 407–415.

Wang, D., Doull, B.A., Oliveira, L.C., Yukihara, E.G., 2013. Controlled synthesis of $Li_2B_4O_7$:Cu for temperature sensing. RSC Adv. 3, 26127–26131.

Wintle, A.G., 1973. Anomalous fading of thermoluminescence in mineral samples. Nature 245, 143–144.

Wintle, A.G., Murray, A.S., 2006. A review of quartz optically stimulated luminescence characteristics and their relevance in single-aliquot regeneration dating protocols. Radiat. Meas. 41, 369–391.

Witkiewicz-Lukaszek, S., Mrozik, A., Gorbenko, V., Zorenko, T., Bilski, P., Fedorov, A., Zorenko, Y., 2020. LPE growth of composite thermoluminescent detectors based on the $Lu_{3-x}Gd_xAl_5O_{12}$:Ce single crystalline films and YAG:Ce crystals. Crystals 10, 189.

Xu, J., Murata, D., Ueda, J., Viana, B., Tanabe, S., 2018. Toward rechargeable persistent luminescence for the first and third biological windows via persistent energy transfer and electron trap redistribution. Inorg. Chem. 57, 5194–5203.

Yanagida, T., Okada, G., Kawaguchi, N., 2019. Ionizing-radiation-induced storage-luminescence for dosimetric applications. J. Lumin. 207, 14–21.

Yeh, S.M., Su, C.S., 1996. Mixing LiF in Gd_2O_3:Eu to enhance ultraviolet radiation induced thermoluminescent sensitivity after sintering process. Mater. Sci. Eng. B 38, 245–249.

Yen, W.M., Shionoya, S., Yamamoto, H., 2007. Phosphor Handbook. CRC Press, Boca Raton, FL.

Yen, W.M., Weber, M.J., 2004. Inorganic Phosphors: Compositions, Preparation and Optical Properties. CRC Press, Boca Raton.

Yoshimura, E.M., Yukihara, E.G., 2006. Optically Stimulated Luminescence: searching for new dosimetric materials. Nucl. Instrum. Methods Phys. Res. B 250, 337–341.

Yuan, L.F., Jin, Y.H., Su, Y., Wu, H.Y., Hu, Y.H., Yang, S.H., 2020. Optically stimulated luminescence phosphors: principles, applications, and prospects. Laser Photon. Rev. 14, 2000123.

Yukihara, E.G., 2011. Luminescence properties of BeO optically stimulated luminescence (OSL) detectors. Radiat. Meas. 46, 580–587.
Yukihara, E.G., 2020. A review on the OSL of BeO in light of recent discoveries: the missing piece of the puzzle? Radiat. Meas. 134, 106291.
Yukihara, E.G., Ahmed, M.F., 2015. Pixel bleeding correction in laser scanning luminescence imaging demonstrated using optically stimulated luminescence. IEEE Trans. Med. Imag. 34, 2506–2517.
Yukihara, E.G., Andrade, A.B., Eller, S., 2016. BeO optically stimulated luminescence dosimetry using automated research readers. Radiat. Meas. 94, 27–34.
Yukihara, E.G., Christensen, J.B., Togno, M., 2022a. Demonstration of an optically stimulated luminescence (OSL) material with reduced quenching for proton therapy dosimetry: MgB_4O_7:Ce,Li. Radiat. Meas. 152, 106721.
Yukihara, E.G., Coleman, A.C., Bastani, S., Gustafson, T., Talghader, J.J., Daniels, A., Stamatis, D., Lightstone, J.M., Milby, C., Svingala, F.R., 2015. Particle temperature measurements in closed chamber detonations using thermoluminescence from $Li_2B_4O_7$:Ag,Cu, MgB_4O_7:Dy,Li and $CaSO_4$:Ce,Tb. J. Lumin. 165, 145–152.
Yukihara, E.G., Coleman, A.C., Biswas, R.H., Lambert, R., Herman, F., King, G.E., 2018. Thermoluminescence analysis for particle temperature sensing and thermochronometry: principles and fundamental challenges. Radiat. Meas. 120, 274–280.
Yukihara, E.G., Coleman, A.C., Doull, B.A., 2014a. Passive temperature sensing using thermoluminescence: laboratory tests using $Li_2B_4O_7$:Cu,Ag, MgB_4O_7:Dy,Li and $CaSO_4$:Ce,Tb. J. Lumin. 146, 515–526.
Yukihara, E.G., Doull, B.A., Gustafson, T., Oliveira, L.C., Kurt, K., Milliken, E.D., 2017. Optically stimulated luminescence of MgB_4O_7:Ce,Li for gamma and neutron dosimetry. J. Lumin. 183, 525–532.
Yukihara, E.G., McKeever, S.W.S., 2011. Optically Stimulated Luminescence: Fundamentals and Applications. John Wiley & Sons, Chichester, West Sussex, UK.
Yukihara, E.G., McKeever, S.W.S., Andersen, C.E., Bos, A.J.J., Bailiff, I.K., Yoshimura, E. M., Sawakuchi, G.O., Bossin, L., Christensen, J.B., 2022b. Luminescence dosimetry. Nat. Rev. Methods Primers 2 (26), 1–21.
Yukihara, E.G., Milliken, E.D., Doull, B.A., 2014b. Thermally stimulated and recombination processes in MgB_4O_7 investigated by systematic lanthanide doping. J. Lumin. 154, 251–259.
Yukihara, E.G., Milliken, E.D., Oliveira, L.C., Orante-Barrón, V.R., Jacobsohn, L.G., Blair, M.W., 2013. Systematic development of new thermoluminescence and optically stimulated luminescence materials. J. Lumin. 133, 203–210.
Yukihara, E.G., Mittani, J.C.R., Vanhavere, F., Akselrod, M.S., 2008. Development of new optically stimulated luminescence neutron dosimeters. Radiat. Meas. 43, 309–314.
Yukihara, E.G., Ruan, C., Gasparian, P.B.R., Clouse, W.J., Kalavagunta, C., Ahmad, S., 2009. An optically stimulated luminescence system to measure dose profiles in X-ray computed tomography. Phys. Med. Biol. 54, 6337–6352.
Yukihara, E.G., Whitley, V.H., McKeever, S.W.S., Akselrod, A.E., Akselrod, M.S., 2004. Effect of high-dose irradiation on the optically stimulated luminescence of Al_2O_3:C. Radiat. Meas. 38, 317–330.
Yukihara, E.G., Whitley, V.H., Polf, J.C., Klein, D.M., McKeever, S.W.S., Akselrod, A.E., Akselrod, M.S., 2003. The effects of deep trap population on the thermoluminescence of Al_2O_3:C. Radiat. Meas. 37, 627–638.
Yukihara, E.G., Yoshimura, E.M., Lindstrom, T.D., Ahmad, S., Taylor, K.K., Mardirossian, G., 2005. High-precision dosimetry for radiotherapy using the optically stimulated luminescence technique and thin Al_2O_3:C dosimeters. Phys. Med. Biol. 50, 5619–5628.
Yukihara, E.G., Yoshimura, E.M., Okuno, E., 2002. Paramagnetic radiation-induced defects in gamma-irradiated natural topazes. Nucl. Instrum. Methods Phys. Res. B 191, 266–270.
Zhang, B., Xu, X., Li, Q., Wu, Y., Qiu, J., Yu, X., 2014. Long persistent and optically stimulated luminescence behaviors of calcium aluminates with different trap filling processes. J. Solid State Chem. 217, 136–141.
Zhao, Y., Wang, Y., Jin, H., Yin, L., Wu, X., Ma, Y., Townsend, P.D., 2019. Thermoluminescence spectra of rare earth doped magnesium orthosilicate. J. Alloys Compd. 797, 1338–1347.
Zhydachevskii, Y., Luchechko, A., Maraba, D., Martynyuk, N., Glowacki, M., Bulur, E., Ubizskii, S., Berkowski, M., Suchocki, A., 2016. Time-resolved OSL studies of $YAlO_3$:Mn^{2+} crystals. Radiat. Meas. 94, 18–22.
Zhydachevskii, Y., Suchocki, A., Berkowski, M., Bilski, P., Warchol, S., 2010. Characterization of $YAlO_3$:Mn^{2+} thermoluminescent detectors. Radiat. Meas. 45, 516–518.
Zhydachevskii, Y., Suchocki, A., Berkowski, M., Zakharko, Y., 2007. Optically stimulated luminescence of $YAlO_3$:Mn^{2+} for radiation dosimetry. Radiat. Meas. 42, 625–627.
Zverev, D.G., Vrielinck, H., Goovaerts, E., Callens, F., 2011. Electron paramagnetic resonance study of rare-earth related centres in K_2YF_5:Tb^{3+} thermoluminescence phosphors. Opt. Mater. 33, 865–871.